1996

Synthesis of Novel Amino Acids With Incorporation Into Peptides and Synthesis of Peptides With Novel Aggregation States.

Scott Michael Cowell
Louisiana State University and Agricultural & Mechanical College

INFORMATION TO USERS

This manuscript has been reproduced from the microfilm master. UMI films the text directly from the original or copy submitted. Thus, some thesis and dissertation copies are in typewriter face, while others may be from any type of computer printer.

The quality of this reproduction is dependent upon the quality of the copy submitted. Broken or indistinct print, colored or poor quality illustrations and photographs, print bleedthrough, substandard margins, and improper alignment can adversely affect reproduction.

In the unlikely event that the author did not send UMI a complete manuscript and there are missing pages, these will be noted. Also, if unauthorized copyright material had to be removed, a note will indicate the deletion.

Oversize materials (e.g., maps, drawings, charts) are reproduced by sectioning the original, beginning at the upper left-hand corner and continuing from left to right in equal sections with small overlaps. Each original is also photographed in one exposure and is included in reduced form at the back of the book.

Photographs included in the original manuscript have been reproduced xerographically in this copy. Higher quality 6" x 9" black and white photographic prints are available for any photographs or illustrations appearing in this copy for an additional charge. Contact UMI directly to order.

UMI

A Bell & Howell Information Company
300 North Zeeb Road, Ann Arbor MI 48106-1346 USA
313/761-4700 800/521-0600

SYNTHESIS OF NOVEL AMINO ACIDS WITH INCORPORATION INTO PEPTIDES AND SYNTHESIS OF PEPTIDES WITH NOVEL AGGREGATION STATES

A Dissertation

Submitted to the Graduate Faculty of the
Louisiana State University and
Agricultural and Mechanical College
in partial fulfillment of the
requirements for the degree of
Doctor of Philosophy

in

The Department of Chemistry

By

Scott M.Cowell
B.A University of Alabama in Huntsville, 1989
December 1996

Table of Contents

List of Tables

List of Figures

Abstract

Peptides exhibit properties based on the amino acids present in the peptide and structure the peptide assumes in its environment. For example, peptides have been shown to be antimicrobial when they are amphipathic and in an α-helical shape. The mechanism for this antimicrobial activity is subject to dispute. One theory states that the peptides work by forming a "pore" through the cell membrane which causes a depolarization of the membrane and the cell lysis because of osmosis. Another theory states that the peptides merely compromise the integrity of the membrane by solubilizing the membrane.

In order for the "pore" theory of lytic activity to occur, the peptides must arrange themselves in a discrete aggregated fashion. The goal of this research is to explore the nature of the aggregated state of designed peptides through the use of CD spectroscopy and fluorescent labeling.

Several peptides were designed using a minimalist approach and were measured using CD spectroscopy to explore how the placement of leucines in the peptides cause a change in their propensity for aggregation. Using this information, the site for an incorporation of a fluorescently labeled peptide was chosen.

The synthesis of the fluorescently labeled amino acid presented an opportunity to explore different types of glycine templates and to find a quicker method for making the amino acid in high yields. After the synthesis of the amino acid, it was incorporated into the peptides and CD and fluorescence studies were accomplished. The result shows the peptides, when aggregated, align themselves in an antiparallel fashion.

1.1 Introduction

The use of antibiotics has caused a general increase in the good health of the people of the world. However, the microbes for which these antibiotics are intended have been slowly building resistance. This has caused a general alarm in the medical field and has spurred research into finding alternatives to the traditional antibiotics. One such alternative has been the use of lytic peptides which can selectively destroy microbes. However, the mechanism by which they destroy pathogens is in dispute. This thesis will attempt to explain the mechanism of interaction while designing novel lytic peptides for possible drug use.

1.2 Definition of Amphipathicity and Aggregation

Some peptides possess the ability to be amphipathic when in an α-helical form. An amphipathic α-helix has all the polar residues aligned on one side of the α-helical axis. Figure 1.2.1 shows a side view of an amphipathic peptide in an α-helical conformation while Figure 1.2.2 shows a longitudinal view of an amphipathic α-helix.

Amphipathic peptides may aggregate. This is best described with this idea of solubility. In an aqueous environment, an amphipathic peptide will want to associate, or aggregate, with another peptide in order for the nonpolar residues of the peptides to solubilize one another. In the case of an aqueous environment, the nonpolar portion of the peptide will be sequestered within the peptide aggregate while the polar portions will be sequestered on the exterior of the peptide aggregate. Figure 1.2.3 shows four amphipathic α-helical peptides aggregated in an aqueous environment.

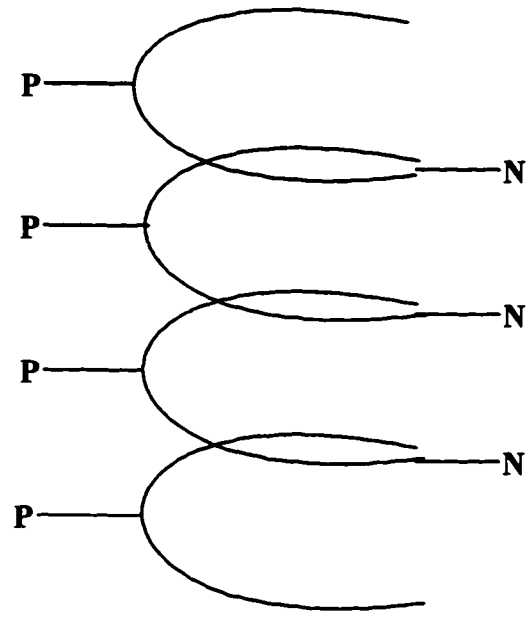

Figure 1.2.1: Side view of an amphipathic α-helix P represents polar residues while N represents nonpolar residues

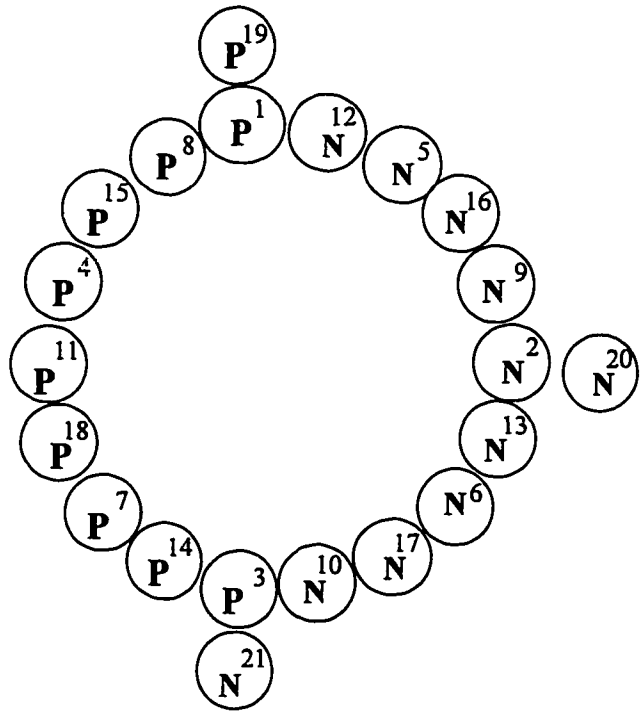

Figure 1.2.2: Longitudinal view of an amphipathic α-helical peptide where P represents Polar residues while N represents Nonpolar residues

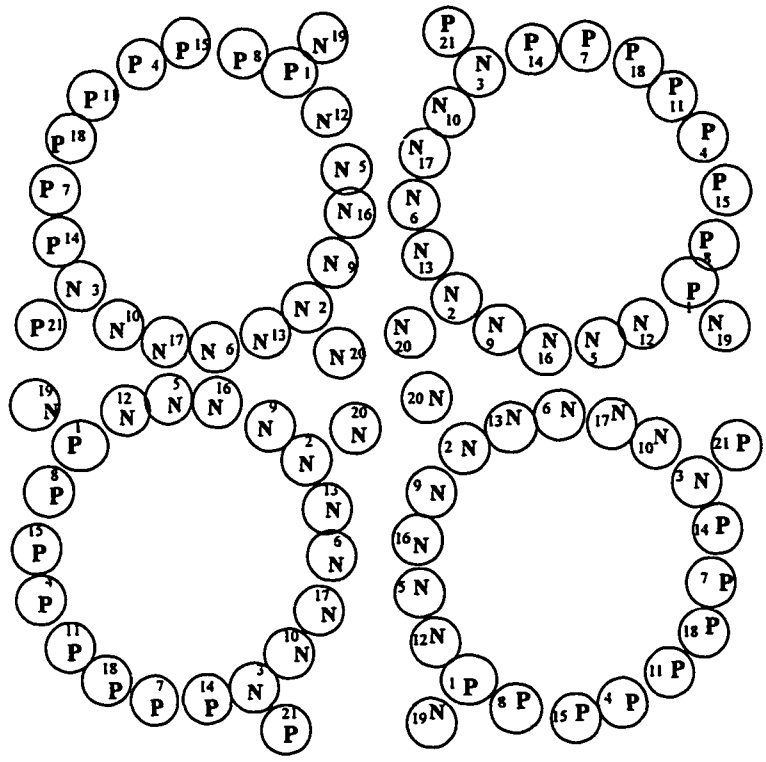

Figure 1.2.3: Representation of an aggregated amphipathic α-helical peptide in an aqueous environment P represents Polar residues while N represents Nonpolar residues

An analogous peptide aggregate can form in a membrane. If four peptides aggregate in a membrane, all the positive charges are on the inner part of the assembly while the nonpolar residues of the peptides interact with the nonpolar regions on the membrane. Figure 1.2.4 represents four peptides aggregating in an membrane environment where P represents polar residues and N represents nonpolar residues. This is one theory which addresses the lytic properties of an amphipathic peptide. The peptide's polar 'inner circle' provides an aqueous environment which can span the hydrophobic part of the membrane. The aqueous environment allows water and ions to freely flow to the cytoplasm of the cell, depolarizing the membrane and causing the cell to rupture. Because of the ability of amphipathic peptides to lyse cells, nature uses them as part of noncellular immune response. Two of these types of peptides discovered are Melittin and Cecropin.

1.3 Melittin

1.3.1 Discovery and Physical properties

Melittin, a lytic peptide isolated from the venom of the bee *Apis mellifera*[1], consists of 26 amino acids with a highly basic C-terminus region with a net charge of 6+ and a hydrophobic N-terminus region. It contains four separate parts: N-terminus α-heix, the flexible "hinge" region, the central α-helix and the positively charged C-terminus region [2].

When in an α-helical shape, melittin has the property of amphipathicity; the polar region will align mostly on one side of the peptide while the nonpolar region will

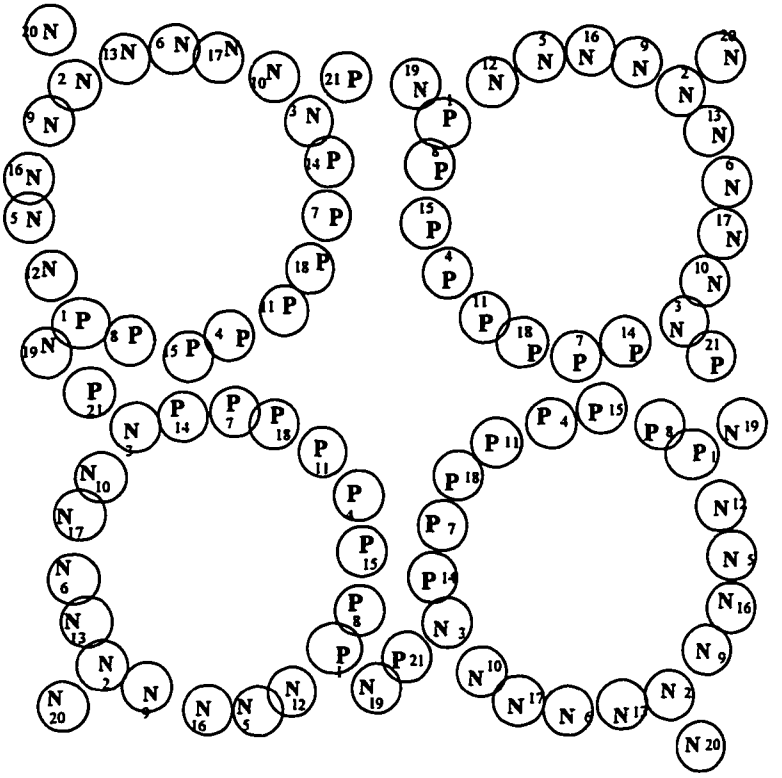

Figure 1.2.4: Representation of the amphipathic α-helical peptides in an membrane environment. P represents Polar residues while N represents nonpolar residues

be on the opposite side of the side of the peptide (see figure 1.3.1). This is not perfectly longitudinal due to the proline-14 located in the center of the peptide. The proline-14 causes a bend in the peptide due to the structure of the amino acid hence the "hinged" region of the peptide.

The amphipathicity of melittin causes the peptide to demonstrate certain properties[1]. Melittin is soluble in aqueous solutions. This solubility causes the hydrophobic region of the amphipathic peptide to aggregate into a tetrameric form. The proximity of the positive charges from the lysines in this self-associated state results in a natural repulsion to self-association. The contribution of charge repulsion in an aggregated peptide, when the charge is increased from +4 to +6 by varying ionic strength, is about 600cal/(charge•mol of tetrameric melittin)[3]. Aggregation can be promoted, or inhibited in melittin by exploiting these contradictory properties.

Anything which suppresses charge formation on the lysine side chains promotes aggregation of the peptides. Solutions with increasing ionic strength promote aggregation by providing a counterion for the (+) charges on the lysines which effectively screen the charge.[1] The nature of the counterion is also a factor in the aggregation of melittin. It has been found that the use of a divalent ion, such as Na_2SO_4, is more effective at promoting aggregation than univalent salts[4]. With the use of Na_2SO_4, Schwarz explored the nature of the formation of tetramers using stop-flow techniques and found that dimerization was the slow step in aqueous self-association, while dimer-dimer interactions to form tetramers were diffusion controlled[4]. However the use of multivalent ions is questioned since multivalent ions form tight interactions with the peptide which are not compatible with helix formation [5].

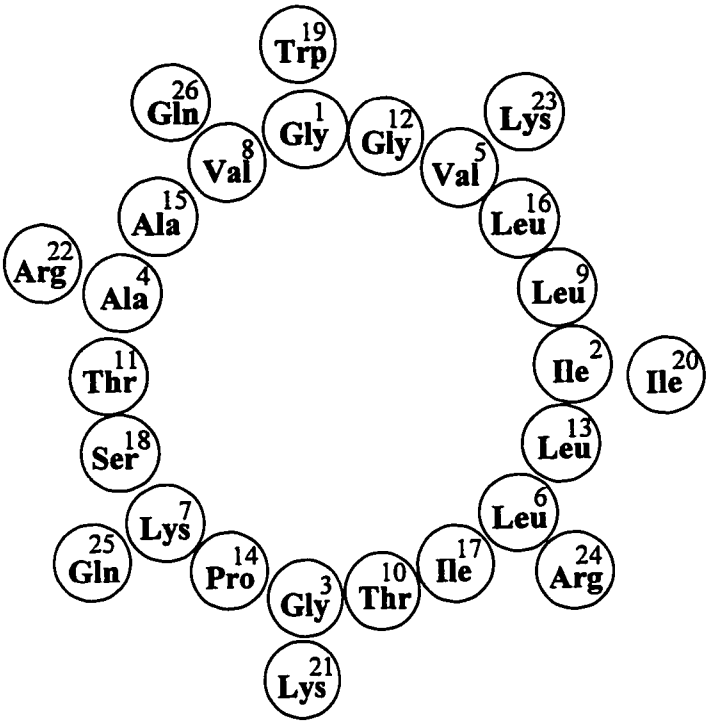

Figure 1.3.1: Edmundson Helical wheel of Melittin

Aggregation is also promoted by changing the pH [1]. By increasing the pH of the aqueous solution, the lysine side chains are deprotonated, reducing charge and promoting aggregation. Since melittin has three ε-amino [Lys-7, Lys-21, Lys-23] and two ε-guanidine [Arg-22, Arg-24] titratable groups, the stepwise titration has been reported.[5] The ionic strength of a solution factors into the influence of the pH on melittin. It has been found that there are two stepwise alkaline transitions when melittin starts at low ionic strength and three at high ionic strength.

A study was also done to explore the charge type vs. α-helicity of the melittin. In one case, a negatively charged analogue of melittin was synthesized and the α-helicity of the melittin analogue was then measured in varying pH, ionic strength and temperature CD studies.[6] A marked decrease in the α-helix propensity of anionic melittin was noted in all conditions. The authors postulated that this was due to the fact that negative charges were in closer proximity compared to the analogous positive charges on melittin. This therefore increased the helix-breaking propensity of the polar region of melittin.[6]

1.3.2 Determination of structure via NMR and crystallography

The structure of melittin was determined by high-resolution NMR spectroscopy. In methanol it was found to adopt an α-helical monomeric form.[1] This study also showed that there was a relaxation of the α-helicity around the Leu-13-pro-14 region due to the 'bending' nature of the proline. The regions of α-helicity had characteristic NOE's while it was noted that towards the end of the peptides, the NOE's were not as prevalent. The conclusion was that the α-helicity of melittin was more relaxed at the ends than in the center of the peptide with the exception of the region that contains the

proline. Melittin was also crystallized in an medium of high ionic strength and the X-ray crystal structure was solved. Under these conditions, melittin adopts an α-helical conformation.[1]

1.3.3 Theories for the mechanism of lytic activity of Melittin

The mechanism of hemolytic activity of melittin is subject to debate. One theory suggests that melittin binds to the surface of a membrane. It then buries into the surface of the membrane through hydrophobic interaction. When four peptides are similarly buried and in proximity to one another, it forms a transmembrane pore which causes lysis via depolarization of the membrane and subsequent osmotic pressure. Figure 1.3.2 illustrates this mechanism.

Another theory about the hemolytic activity of melittin is that the membrane permeability of the peptides cause destruction by micellization of patches of the membrane.[1] This is similar to detergent solubilization. The binding of the peptide and burying of the peptide into the membrane is similar to that of the pore formation theory. Figure 1.3.3 illustrates this mechanism. Evidence for both theories will be presented in the following sections.

1.3.4 Voltage dependence and the pore mechanism for lytic activity

Melittin shows evidence of a pore formation in a membrane with an applied voltage gradient.[1] The application of a potential across a membrane in the presence of a critical concentration of melittin shows a depolarization of the membrane caused by Na^+ ion permeability. Depolarization of the membrane increases in a stepwise fashion as the fourth order of melittin concentration. This indicates that the melittin is coming together in a tetrameric form [1].

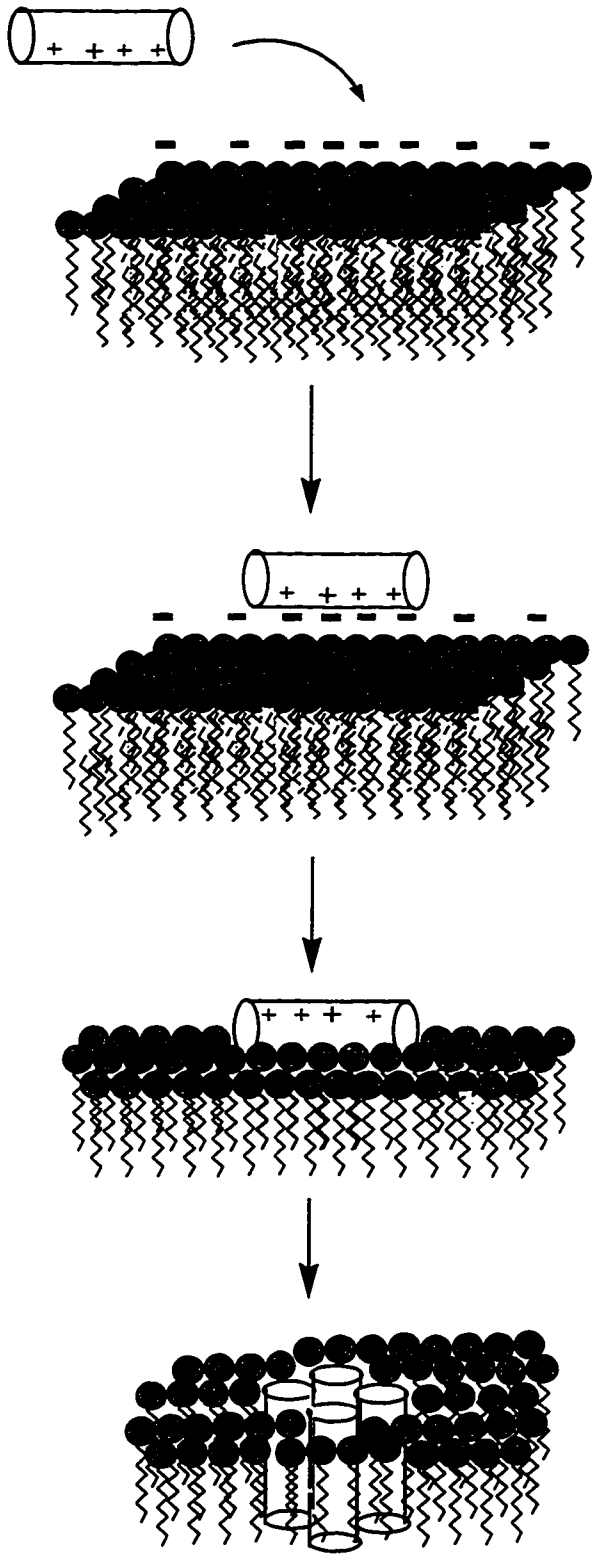

Figure 1.3.2: Mechanism for Melittin pore formation via the "pore" method

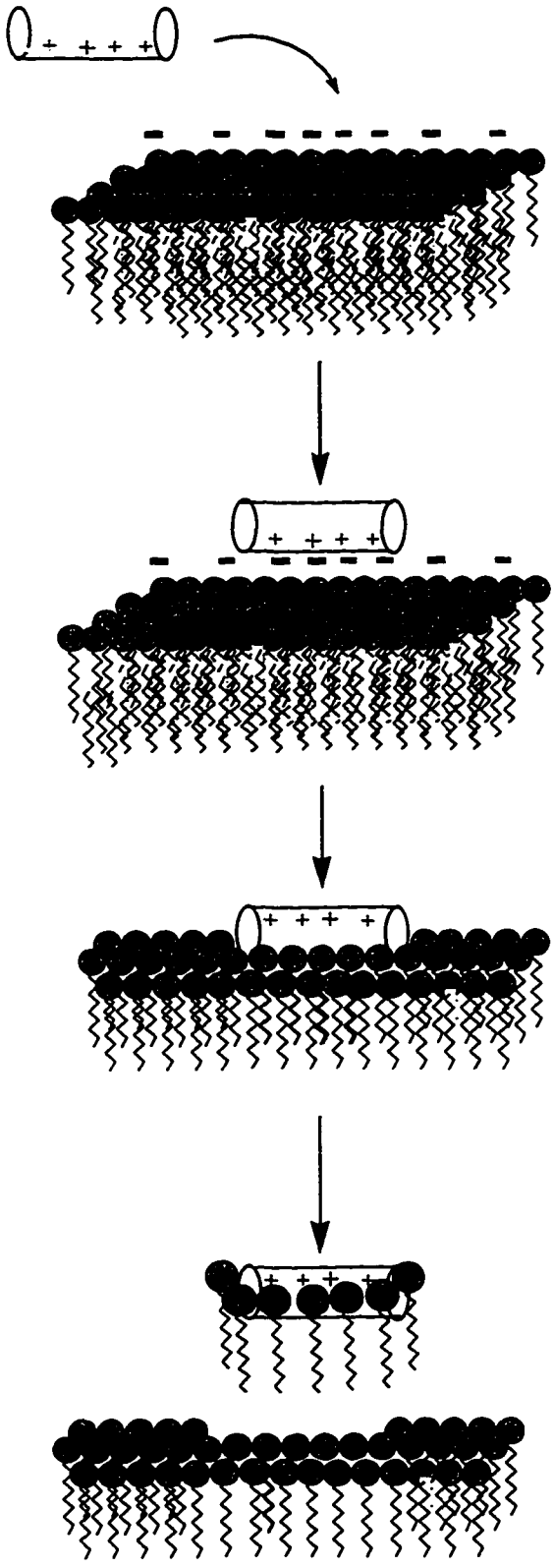

Figure 1.3.3: Mechanism of Melittin "rafting" formation

1.3.5 Effects of lipid concentration

The binding efficiencies of melittin to different types of membranes have also been studied. Many studies have been done on the nature and binding affinities of melittin to various micelles and membranes. Because of the amphipathicity of melittin, the hydrophobic region of melittin interacts with the lipid membrane. Membranes tend to promote α-helical secondary structure in melittin through hydrophobic interaction and melittin was found to bind to a membrane as a monomer.[1] The binding of melittin to a membrane was studied as a function of pH and it was determined that binding increased at increased pH.[7] Increased pH decrease the amount of charge on the lysines causing easier binding to the membranes.

Studies have been done to determine the orientation of the peptide in a membrane after it has bound to the membrane. Determining the orientation of melittin by fluorescence of the tryptophan showed that the tryptophan orientation existed to two forms: it was either embedded in the hydrophobic membrane close to the phospholipid headgroups, or it was exposed to the solvent system[8].

The binding efficiencies of melittin to phophatidylglycerol/phosphatidylcholine membrane showed that there is a greater binding efficiency to this membrane due to presence of negative charges on the membrane [9]. Melittin, in this type of membrane, also reoriented it. The presence of extra negative charge in the membrane caused the N+ charges of the phosphatidylcholine to orient towards the hydrophobic regions. The addition of melittin caused the N+ charges to reorient towards the aqueous media. This is found in the addition of melittin to phosphatidylcholine membranes. Melittin was also introduced to membranes which contain unsaturated tail groups [10]. It was found

that there was a faster leakage of contents in the membrane containing unsaturated bonds. The authors speculated that was not due to the nature of the membrane, but because of the perturbation of the melittin in the membrane. Binding studies of melittin were also done on reversed micelles [11]. Again it was found that melittin binds to the hydrophilic surface of reversed micelles and that it binds in a monomer form.

The binding of melittin caused leakage of the membranes without the presence of a voltage gradient at lytic concentrations is evidence that lytic activity could be caused by the solubilization of the membrane.

1.4 Cecropin

1.4.1 Physical properties of cecropin and analogues

Cecropin A, a peptide isolated from the *Hylophora cecropia* moth, acts as the moth's immune system [12]. The same moth contained cecropin-like peptides subsequently named cecropin B[13] and cecropin D [14] which Merrifield synthesized by via solid phase peptide synthesis. Merrifield first synthesized a fraction of the cecropin A peptide consisting of the first 33 residues. [15] This synthetic peptide proved only slightly less effective as an antimicrobial peptide than the full length peptide.

All the cecropins share certain similarities. They consist of 31 and 39 amino acids, have strongly basic hydrophilic regions near the N-terminus and hydrophobic regions near the C-terminus.[13] These two regions are separated by a central part that contains the α-helix breaking sequence of glycine and proline. An Edmundson helical wheel of Cecropin A, consisting of 37 amino acids is shown in figure 1.4.1. The structure of the peptides were determined by NMR and CD to have α-helical character in 15% HFIP.[16]

A cecropin analogue has also been isolated in mammals. The analogous peptide, named cecropin P1, was isolated from pig intestine. Because of this discovery, Boman theorizes that cecropin like peptides may be present in other mammals as a means of regulating bacterial growth in animals.[17] Though analogous to the other cecropins, cecropin P1 does not contain the central α-helix breaking sequence of glycine and proline common to the other cecropins.[18]

1.4.2 Aggregation of Cecropin

Cecropins has an amphipathic α-helical structure with the polar region containing predominantly positive charges. Consequently hydrophobic interactions of the α-helix promotes aggregation in neutral conditions, electrostatic repulsion of like-charged amino acids diminish aggregation. Therefore the use of any system, whether pH, ionic strength or fluorinated solvents, that suppresses the charge associated with the peptide and will promote the formation of aggregated peptides. This has been determined with cecropin by CD and ESR [19]. Cecropin AD, a hybrid of cecropin A and cecropin D, aggregated in the presence of 5-10% (v/v) HFIP. The researches also showed that increasing the concentration of cecropin in 5-10% HFIP does not increase aggregation. Moreover, decreasing the concentration in the above conditions does not have any effect on the monomer- aggregate equilibrium[19]. The peptides also exhibited aggregate formation in the presence of high salt concentration (1.0 M NaCl) and high pH [19].

1.4.3 Voltage dependent ion channel formation.

Cecropin, at antimicrobial concentrations, formed channels through planar lipid membranes with a negative potential across the membrane. Channel formation is

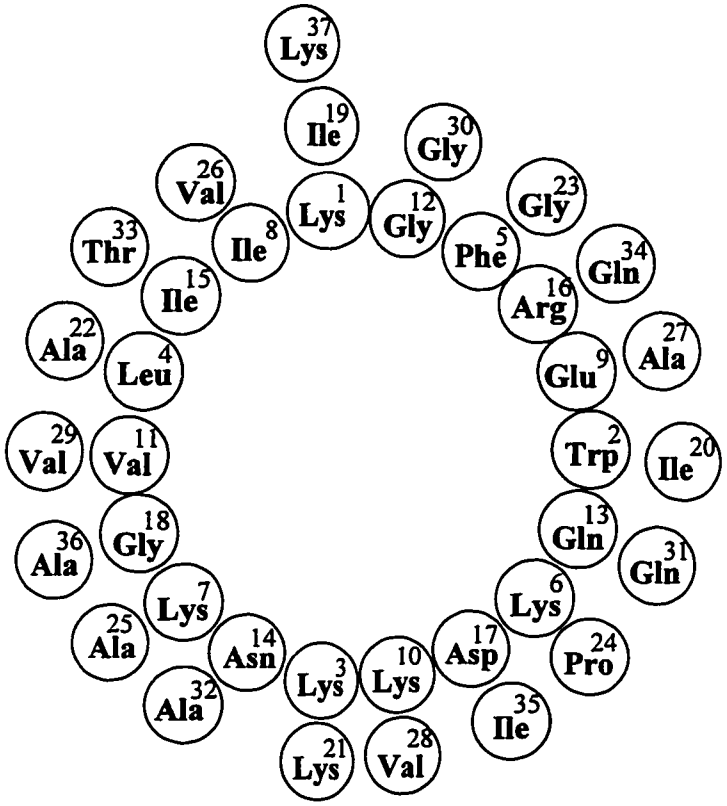

Figure 1.4.1: Edmundson Helical wheel of Cecropin A

decreased in analogous peptides which do not have the hinged region present [20]. The authors suggest that the insertion of the hydrophobic region of the amphipathic peptide and subsequent channel formation is dependent on the hinged region of the peptide. However the central hinged region is not necessary for lytic activity since it is not present in cecropin P1[18]. Molecular modeling found that cecropin possesses the possibility of two types of transmembrane pores [21]. Without an applied potential, the predicted pore forms with the nonpolar C-terminus buried in the lipid bilayer while the hydrophilic N-terminus is associated with the phospholipid headgroups. While with an applied potential, the ion channel is formed with the hydrophilic N-terminus group actually forming the channel. This hypothesis is not supported by experimental data.

1.4.4 Interactions of Cecropin with lipid bilayers

The controversy over the mechanism of action of lytic activity, by pore formation or membrane permeability, exists for cecropins. The cecropins seem to bind to a lipid bilayer as a monomer. Cecropin B2, a cecropin derivative isolated from the silkworm *Bombyx moris,* supposedly causes disintegration of the membrane leading to membrane permeation [22]. This was determined by the use of spectroscopic dyes placed on the cecropin B2. The concentration of cecropin needed to lyse the liposome can be correlated with the amount needed to lyse a bacteria and it was concluded that cecropin coats the bacteria before lysis occurs [Merrifield, 1988 #157]. However, the study was done on neutral liposomes. It is possible that on a neutral membrane, the action involving membrane permeation is possible while on a membrane containing a distinct potential, the pore formation is predominant.

1.5 Modifications on naturally occurring peptides

The use of Cecropin as a possible antibiotic proves to be cost prohibitive due to the length of the peptide. Melittin, on the other hand, is smaller and less costly to produce, but its property of lysing erythrocytes makes it useless as a drug. Therefore scientists have experimented with hybrids in order to combine the broad spectrum antibiotic character of the cecropins with the shorter length of melittin while trying to suppress melittin's property of lysing erythrocytes.

One of the first hybrids synthesized was the combination of Cecropin A and Cecropin D [23]. This consisted of combining the amino acids 1-11 of cecropin A with amino acids 12-37 of Cecropin D. From this study, Fink and coworkers confirmed the importance of the highly basic amphipathic α-helix have in the antimicrobial activity. With this, more ambitious hybrids were made in order to decrease the size of the peptides.

The first highly successful peptide hybrid combined the basic residues of cecropin A (1-13) with the hydrophobic residues of melittin (1-13) [24]. The result was better antibacterial activity compared to the parent peptides even when their overall size was decreased to 26 amino acids which represents a 30% decrease compared to cecropin[24]. Figure 1.5.1 shows a table comparing the antimicrobial activity of the parent peptides with various hybrids of cecropin and melittin. The authors were trying to follow the basic structural components found in the lytic peptides which are a basic amphipathic α-helix, a flexible segment between helices and a hydrophobic α-helix[24]. Manipulation of the peptide sequence showed that the removal of the Gly Pro hinge region caused an overall increase in bioactivity[24]. The NMR showed that the peptide

forms an α-helical structure[25]. Throughout the studies, the authors assumed that the mechanism for lytic activity was due to pore formation. They then concluded that the minimum length for the peptide to span the membrane was 20 amino acids long. This, however, was soon proven false.

The authors continued to do research on the CA(1-13)M(1-13) peptide. By deleting amino acids from the hydrophobic melittin like region of the hybrid, they showed that even 15 amino acid peptide hybrids have lytic activity[26]. This finding caused a revision of the theory of pore formation as the mechanism of action in the peptide. It is interesting to note the CD studies done on these peptides. Merrifield showed that the peptides that were 18 and 20 amino acids long contained some β-sheeting in 4-12% HFIP with a plateau of 50% helicity at 16-20% HFIP. The small peptides were observed to have a high α-helix content at only 12% HFIP. This was attributed to the absence of the Gly-Ile-Gly-Ala which disrupts the helix continuity[25].

With these findings, the authors decided that pore formation may be accomplished by noncovalent dimerization of the peptides to span the membrane or through a 3_{10}-helix formation[25].

Table 1.4.1: Lytic Activity of Parent Peptides and Peptide Hybrids in μM CA, CecropinA; M, Melittin; EC, *Escherichia coli*; PA, *Pseudomonas aeruginosa*; SA, *Staphylococcus aureus*; SRC, sheep red blood cells

Parent Peptides	EC	PA	SA	SRC
Cecropin A (1-37)	0.2	4	>200	>200
Melittin (1-26)	0.8	0.2	0.2	4-8
Hybrid Peptides				
CA(1-24)M(1-13)	0.3	0.5	6	>200
CA(1-13)M(1-13)	0.5	0.7	2	>200
CA(25-37)M(1-13)	200	20	>300	>300
M(1-13)CA(1-13)	1	0.3	5	80
M(16-26)CA(1-13)	0.7	0.7	10	>200

2.1 De Novo Peptide design

Studies have shown that sequence homology is not prerequisite for biological activity as long as the peptide remains amphipathic and is of sufficient length [27]. Simplified analogs of natural peptides that retain or enhance helix amphipathicity and "minimalist" de novo designed amphipathic helix peptides have lytic activity[28]. The purpose of the research accomplished was to design antimicrobial peptides using a "minimalist" approach. The goal was to incorporate features found in nature with recent advances in de novo design to form peptides that were both antimicrobial and gave information concerning the mechanism of interaction of the peptides. The design of the peptides were based on the "pore" theory of their mechanism in which the lytic activity of the peptides occurred due to the formation of a pore across the membrane which depolarizes the membrane and causes subsequent lysing. In order for this to occur, in our design structure, one had to make the peptides so that they possessed the possibility to aggregate in a certain fashion. Hence the peptides had to be amphipathic when in an α-helical structure and leucines were used in the hydrophobic region to ensure that aggregation could occur.

An aspect of the design actively explored was the role of the hydrophilic face of the peptides. This was based on the idea that the degree arc of the hydrophilic face could affect how the peptides would aggregate in a membrane. By having a large degree arc, one would expect a larger pore to form while having a smaller degree arc, one would have a smaller pore form. If the actual size of the pore could not be affected, then the ease of aggregation of the pore could be affected by the amount of nonpolar moiety present in the system.

Another aspect of the antimicrobial peptides was explored concerning the idea of a leucine zipper. Leucine zippers would be used to facilitate the aggregation of the peptides in aqueous environment. With the peptides aggregated into discrete packages in aqueous environment, one could think of this as a form of delivering the peptides to cells in "packages". After initial binding to the cell membrane, the peptide tetramers would then quickly rearrange to a pore formation and lyse the cell. Hence, if the pore model is correct, the peptides would act as their own drug delivery system and less peptide would be needed in order to facilitate a lytic and thus antimicrobial response.

Finally, the peptides were designed in a minimalistic fashion so that, if their use as a drug was possible, the peptides would be easy to mass produce through solution phase synthesis. The peptides were designed as heptad repeats. Heptad repeats have the ability to form descreet amphipathic units while making them easier to produce with solution phase chemistry. Therefore we designed putative lytic peptides consisting of heptad repeats by subdividing the heptad into two identical trimers and an additional residue. To keep the polar and nonpolar faces approximately the same size there are two possibilities: design trimers made from two nonpolar residues, N, and one positively charged residue, P, with an additional positively charged residue, P; or trimers made from one N, two Ps and an additional N. There are nine possible and eight unique combinations of heptads for each of these possibilities. The heptads composed with trimers N,N and P with a P are: (PNN)(PNN)P, (PNN)P(PNN), P(PNN)(PNN), (NNP)(NNP)P, (NNP)P(NNP), (NPN)(NPN)P, (NPN)P(NPN), and P(NPN)(NPN). The latter three heptads are not amphipathic in α-helical conformations and so were not considered further. The peptides that were designed and synthesized can be generalized

as (PNN)(PNN)P and (NNP)P(NNP). This design approach generates a large number of structurally related peptides that differ only in the sequence or that have similar sequences with single amino acid residue replacements at several related sites in a peptide. Figure 2.1.1 shows the two distinct amphipathic peptides generated by the above sequences. These peptide designs encompass all the aspects that was desired which were to be minimalistic and have distinct parameters. The change in the sequence of the designed heptad changed the polar face of the peptdes. This was a source of experimentation to see if the degree-arc of polar face would change the biological activity of the peptides. Finally, the face of the nonpolar aspect of the molecule provided a site for possible aggregation.

2.2 Specific Peptide Design

The amino acids incorporated in the P and N of the above de novo design system were leucines, lysines and alanines. Leucines were used to provide a possible site for aggregation of the peptides. The lysines provide a positively charged amino acid which would be easily incorporated into a peptide and would be easily used on a solid phase peptide synthesis. Finally, the alanines were incorporated because of their ability to promote α-helicity.

The first peptide designed consisted of a heptad of (Lys,Leu,Ala,Lys,Leu,Ala,Lys) repeated three times. It was designed to be a 21 residue peptide in order to assure that it would span a membrane and obtain an α-helical structure under appropriate conditions.

By definition, a leucine zipper can occur when leucines are placed in every seventh position on a peptide chain. Following this rule, the peptides designed will be

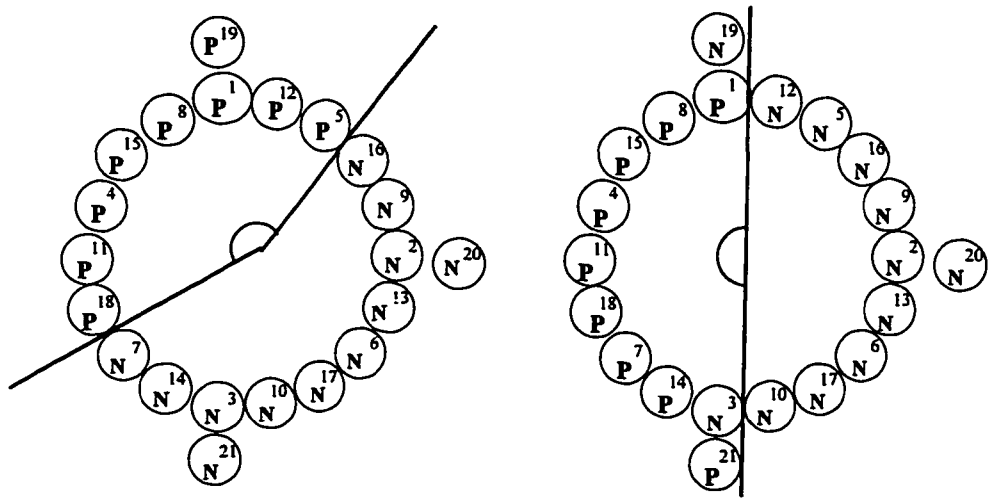

(PNNPNNP) (PNNPPNN)

Figure 2.1.1: Two amphipathic structures generated by the heptad sequences. The left figure represents a 160° polar face while the right figure represents a 180° polar face

capable of forming leucine zippers. The primary leucine zipper has three leucine amino acids spaced so that they will have the ability to aggregate easily. When a peptide assumes an α-helical conformation, it is usually the core of the peptide that will be most helical, while the ends of the peptide will have more random coil character. Therefore, the leucines in the core of the peptide will form a more stable aggregated state and are thus defined as the primary positions. The other leucines, called the secondary system, are four amino acids away from the primary system and help to stabilize the leucine zipper by providing additional hydrophobic character. Figure 2.2.2 represents the Edmundson wheel of this particular peptide. This peptide shows a 180° polar face with a possible leucine aggregation site.

Another peptide was designed to determine whether the peptide activity was sequence dependent. The sequence is (Lys,Ala,Leu,Lys,Ala,Leu,Lys)$_3$ and is very similar to the first sequence presented in this section. another. Consequently the leucine zippers in the primary state will be closer to the lysine polar face of the peptide. The peptide with a 180° polar face is shown figure 2.2.3.

Finally another design consisted of the heptad sequence of (Lys,Leu,Ala,Lys,Lys,Leu,Ala). This demonstrates that by merely changing the sequence of the amino acids, the peptide can have a different polar face in the α-helical structure. In this case, the leucine zipper in the primary position are still adjacent to the lysine polar face of the peptide. The peptide has a 160° polar face and figure 2.2.4 shows the Edmundson helical wheel of the peptide.

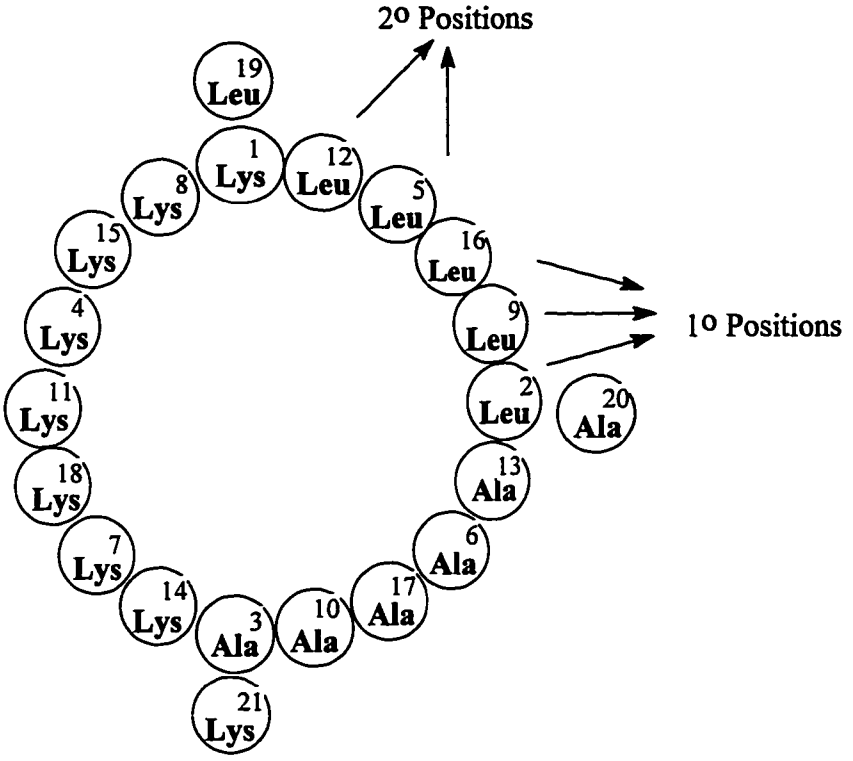

Figure 2.2.2: Edmundson wheel of (Lys,Leu,Ala,Lys,Leu,Ala,Lys)3

To conclude, the peptides were designed to show how changes in the sequence homology of the peptides changes some basic characteristics. All peptides designed in this section have common characteristics. First, they all are designed in the minimalist fashion with the same amino acids used in each peptide and all amphipathic when in an α-helical conformation. They also have the ability to aggregate in a descreet fashion using a phenomena called a leucine zipper. The difference in these peptides result from changes in the sequence homology of the peptides. Due to the changes in the sequence, two peptides have a 180° polar face while the third has a 160° polar face.

2.3 Results and Discussion

2.3.1 Solid Phase Peptide Synthesis

The peptides were all synthesized using a Milligen 9050 peptide synthesizer. As opposed to solution phase peptide synthesis, which couples dipeptides and tripeptides into larger ones, solid phase peptide synthesis couples individual amino acids sequentially in order to form the larger peptide.

Solid phase peptide synthesis uses a solid phase support which is covalently attached to the first amino acid. This anchors the first amino acid as the others are coupled to it sequentially. In this case, polystyrene beads with a polyethylene glycol chain, known as PAL-PEG-PS resin, was used as the solid phase support. The first amino acid is coupled to the resin via an amide link. The amino acids which follow are protected amino acids. The amino acids can have a variety of different protecting groups associated with them. In this methodology, the α-amine on the amino acids were

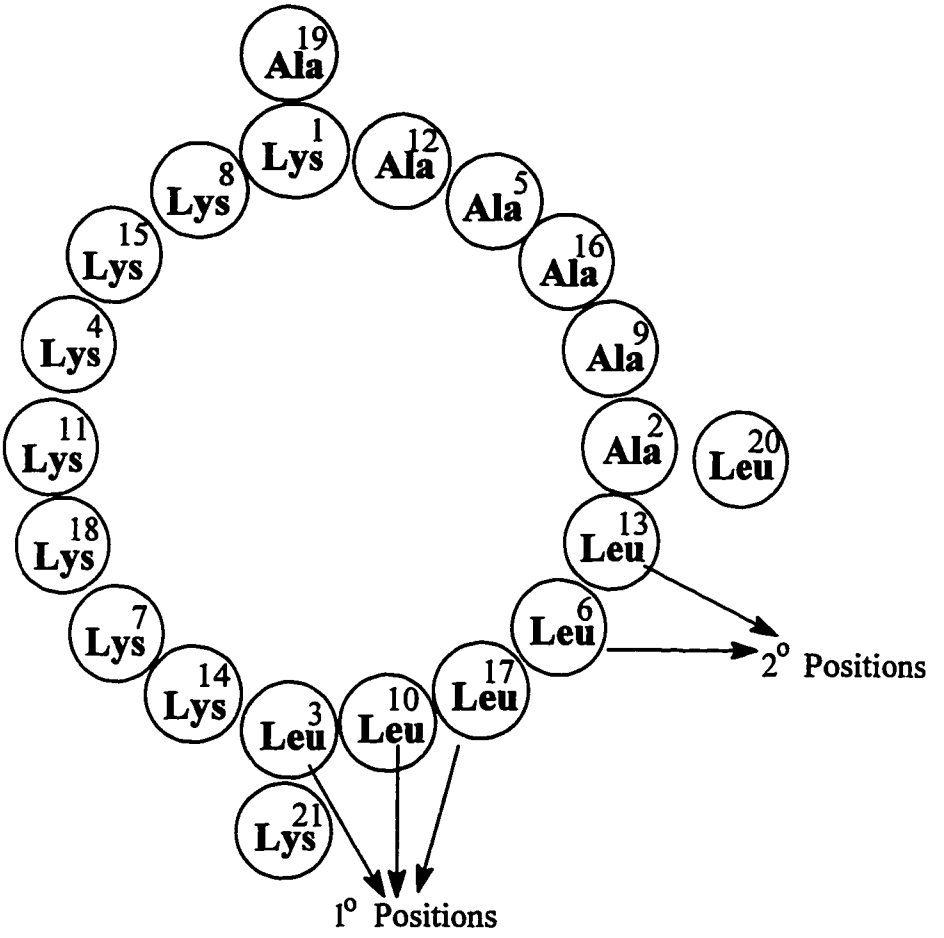

Figure 2.2.3: Edmundson wheel of (Lys,Ala,Leu,Lys,Ala,Leu,Lys)$_3$

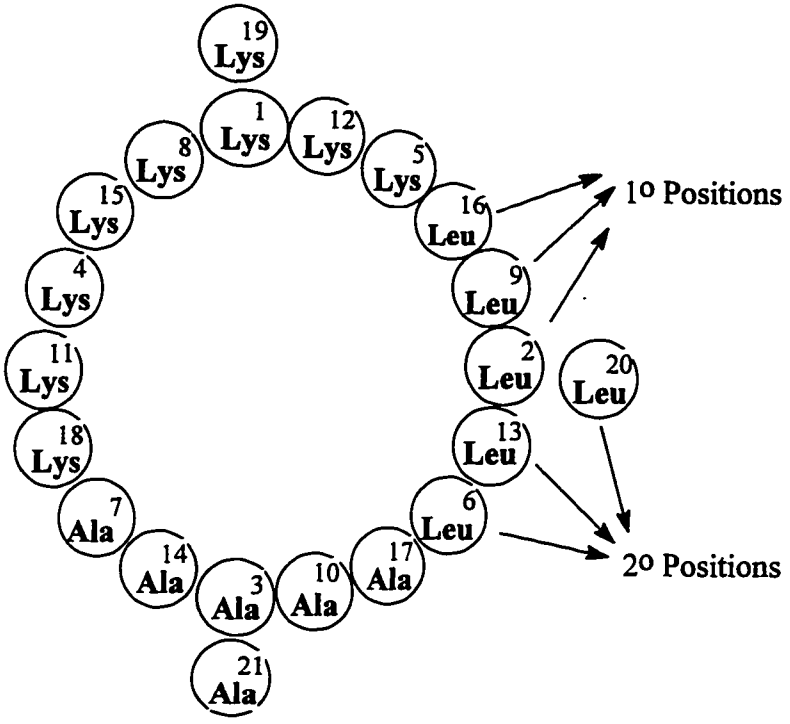

Figure 2.2.4: Edmundson wheel of (Lys,Lue,Ala,Lys,Lys,Leu,Ala)3

protected using fluorenylmethoxycarbonyl (FMOC) while the ε-amine, in the case of the lysine, was protected with tert-butyloxycarbonyl (t-BOC). Two separate protecting groups are used because each protecting group is removed under different conditions, amines protected by FMOC are removed by a base, namely 20% piperidine, while the amines protected by t-BOC are removed by trifluoroacetic acid. These are called orthogonal protecting groups. By using this method, it is possible to deprotect the α-amine while still leaving the ε-amine protected. Finally, the carboxy portion of the amino acid is activated as a pentafluorophenol (Opf) ester.

The sequence of synthesis is as follows. The first amino acid is placed on the Pal-Peg-PS resin via an amide bond. The linked amino acid is then deprotected by a piperidine wash and the next amino acid is linked to it. This cycle is repeated until the desired peptide is made. After the peptide is made, the peptide is cleaved off the resin using TFA. The TFA also deprotects the t-BOC which protected the ε-amine of the lysines. The peptide was purified by two separate methods. Originally the peptides were deprotected using a cleavage cocktail called Reagent B (8.8 mL triflouroacetic acid, 0.5 mL phenol, 0.5 mL water, 0.2 mL of triisopropylsilane). After stirring, the peptide was precipitated out of the cocktail by slowly pouring the peptide/cocktail solution into cold diethyl ether. The purified peptide was centrifuged into a pellet and allowed to dry. The peptide was dissolved in 20% acetic acid and passed through a Sephadex G-15 column to remove any residue of the cleavage cocktail and any very small peptides.

Another method which was employed to purify the peptide was to directly dissolve the peptide/cleavage cocktail in 20% acetic acid and extract the solution in diethyl ether. The 20% acetic acid solution is frozen and lyophilized. The purpose of the diethyl ether extraction was to remove any of the nonpolar organics from the cleavage cocktail. This method also eliminated the need to pass the peptide through a Sephadex G-15 column. Both methods were employed during the synthesis phase of the research and worked equally well.

Due to the nature of solid phase synthesis, if an individual peptide was not successfully deprotected, then there could be failed coupling of the next amino acid. These were separated using RP-HPLC and all three peptides were purified using a RP-HPLC with a C-4 column. The mobile phase was a gradient consisting of water and acetonitrile. Both mobile phases had 0.5% TFA added to insure no bacterial growth and to buffer the solution. Once the conditions of purification were determined and the retention times were noted, a large amount of peptide, approximately 30 mg, was purified using a semi-preparatory C-4 column. A fraction of the purified peptide was rechecked using a C-18 analytical column. Plasma desorption mass spectroscopy was performed to determine if the correct peptide was synthesized.

2.3.2 CD Measurements

A CD study was performed on the peptides to determine the structure as a function of concentration. This study did not use any salt, pH changes, or SDS micelles or vesicles to effect the formation of secondary structure. The study was conducted on the peptides to determine if the influence of the nonpolar portions of the amphipathic α-helix would enforce the α-helix by overcoming the repulsive forces of the charged

amino acids on the peptides. If this was indeed the case and shows how the change in the sequence homology effects helix formation in the peptide.

Of the three peptides, $(Lys,Ala,Leu,Lys,Ala,Leu,Lys)_3$ gave the smoothest transition from a random coil to an α-helical shape. The α-helical CD spectrum is characterized by minima at 208 and 222 nm while random coil has an minima at around 200. If a peptide is going from a random coil to an α-helical secondary structure, then all the CDs of this transition will pass through one point when layed on top of one another. This is called the isodichroic point and is shown in figure 2.3.1.

CD raw data is reported in millidegrees, meaning the degree the polarized light is shifted after it interacts with the peptide. In order to facilitate interpretation, the data is converted to molar ellipticity. This number represents the change in the degree of polarized light per mol of peptide residue. Molar ellipticity is usually calculated at 222nm wavelength of light. This is done using the following formula:

$$[\theta]_{222} = \frac{100^* (\text{milidegrees})_{222}}{1000 * C * L}$$

Where: C= concentration of peptide per residue (Mol)
L= Pathlength of the cell (cm)

After molar ellipticity is determined, % α-helicity for each peptide is determined using the following formula:

$$\% \ \alpha\text{-helicity} = \frac{100^* ([\theta]_{222} + 3000)}{33000}$$

With the above formulas, a table 2.3.2 is generated showing the different molar ellipticities and % α-helicities for each peptide studied.

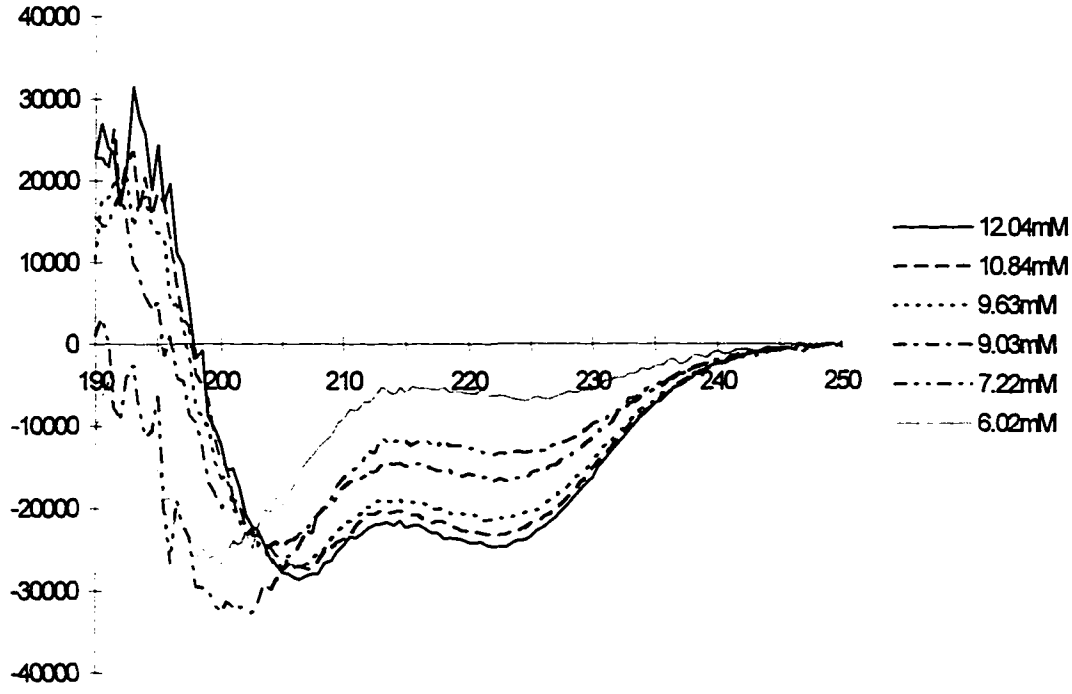

Figure 2.3.1: CD spectra of (Lys,Ala,Leu,Lys,Ala,Leu,Lys)$_3$

Both $(Lys,Leu,Ala,Lys,Lys,Leu,Ala)_3$ and $(Lys,Leu,Ala,Lys,Leu,Ala,Lys)_3$ had similar transitions until the peptide concentration approached log 0.9 to 1.0. The peptide $(Lys,Ala,Leu,Lys,Ala,Leu,Lys)_3$ also had the highest molar ellipticity of -24,887.26 at a log of 1.113 (12.97 mM). The peptide $(Lys,Leu,Ala,Lys,Leu,Ala,Lys)_3$ has a molar ellipticity of -20,101.74 at a log of 1.063 (11.56 mM) while $(Lys,Leu,Ala,Lys,Lys,Leu,Ala)_3$ demonstrated the least propensity of aggregation with a molar ellipticity of -14,249.65 at a log of 1.15 (14.125 mM). Figures 2.3.3 and 2.3.4 represent the CD spectra of $(Lys,Leu,Ala,Lys,Lys,Leu,Ala)_3$ and $(Lys,Leu,Ala,Lys,Leu,Ala,Lys)_3$. Figure 2.3.5 represents a comparison of the molar ellipticity vs. the log of the concentration of the three peptides.

The two peptides which demonstrated the greatest difference in propensity for α-helicity are $(Lys,Leu,Ala,Lys,Lys,Leu,Ala)_3$, and $(Lys,Leu,Ala,Lys,Lys,Leu,Ala)_3$. It is interesting to note that by merely changing the sequence of the amino acids, the propensity for α-helicity is dramatically changed. The explanation for this lies in how the peptides become α-helical. When a peptide is said to be in an α-helical comformation, this doesn't mean that all amino acids are participating equally in the α-helix. In fact, as demonstrated by melittin, the ends of the peptide still stay in a random coil conformation. α-Helicity does not actually start until the third residue of the peptide. The peptide $(Lys,Ala,Leu,Lys,Ala,Leu,Lys)_3$ has the highest propensity for aggregation due to the primary leucine zipper. As shown on figure 2.2.3, the primary leucine zipper for this peptide starts are on residues 3, 10 and 17. Therefore all of the leucine amino acids are within the α-helical portion of the peptide and can equally

Table 2.3.1: Relative Molar ellipticities and % α-helicities for $(KALKALK)_3$, $(KLAKKLA)_3$, and $(KLAKLAK)_3$

$(KALKALK)_3$

Log [Peptides] mM	Molar Ellipticity	% α-Helicity
0.3784	1957.163	15.022
0.5545	2426.919	16.445
0.6794	5899.582	26.968
0.7763	8584.43	35.104
0.8585	13500.99	50.003
0.9557	16674.05	59.618
0.9836	21367.48	73.841
1.035	23117.42	79.144
1.081	24700.6	83.507
1.113	24887.26	84.507

$(KLAKKLA)_3$

Log [Peptides] mM	Molar Ellipticity	% α-Helicity
0.40926	954.4222	11.9831
0.58535	4687.674	23.296
0.7103	7427.718	31.599
0.80787	7939.197	33.149
0.9212	13121.68	48.8536
0.98399	14293.2	52.404
1.0120	16749.12	59.8458
1.0630	20101.74	70.0052

$(KLAKLAK)_3$

Log [Peptide] mM	Molar Ellipticity	% α-Helicity
0.449	1689.359	14.210
0.625	2873.4	17.798
0.769	5019.697	24.302
0.849	5570.235	25.970
1.025	12088.52	45.723
1.104	14171.35	52.034
1.150	14249.65	52.272

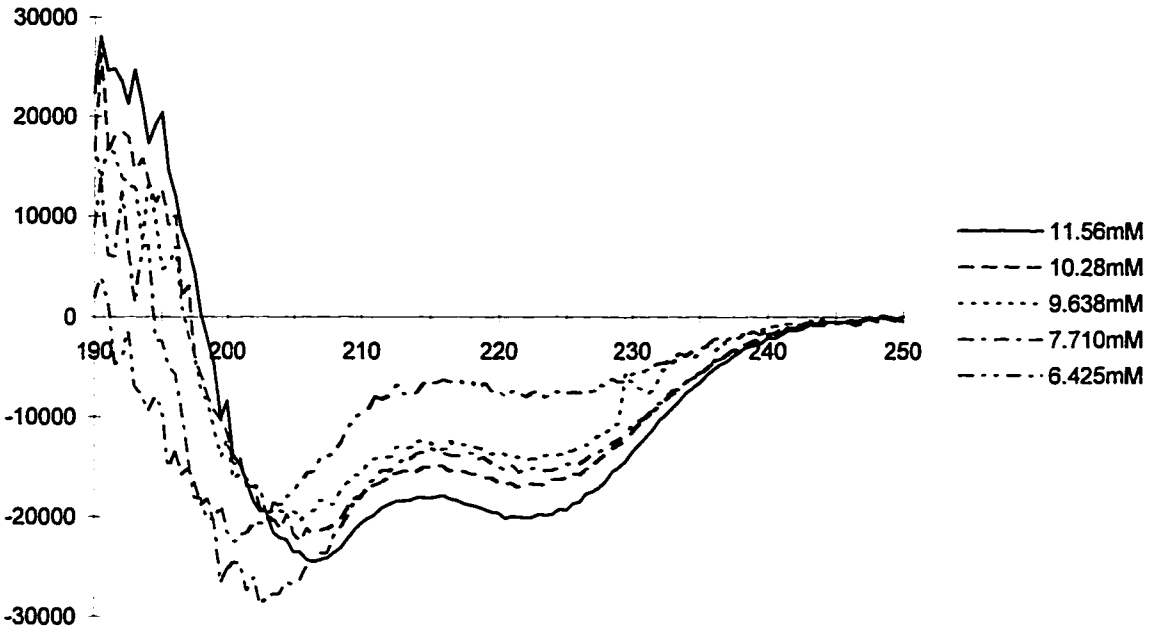

Figure 2.3.2: CD spectra of (Lys,Leu,Ala,Lys,Lys,Leu,Ala)$_3$

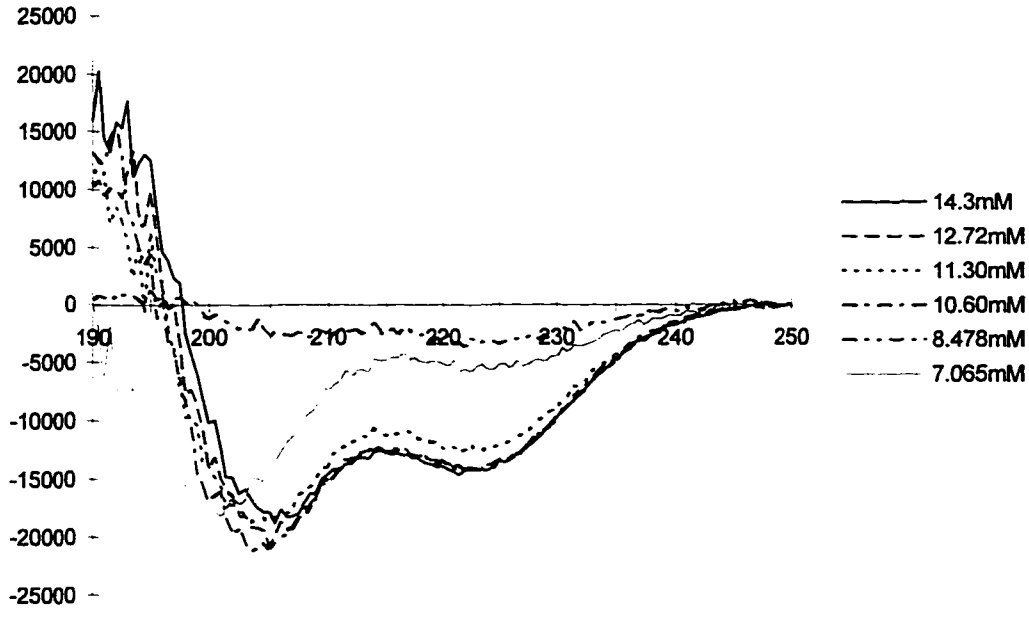

Figure 2.3.3: CD spectra of (Lys,Leu,Ala,Lys,Leu,Ala,Lys)$_3$

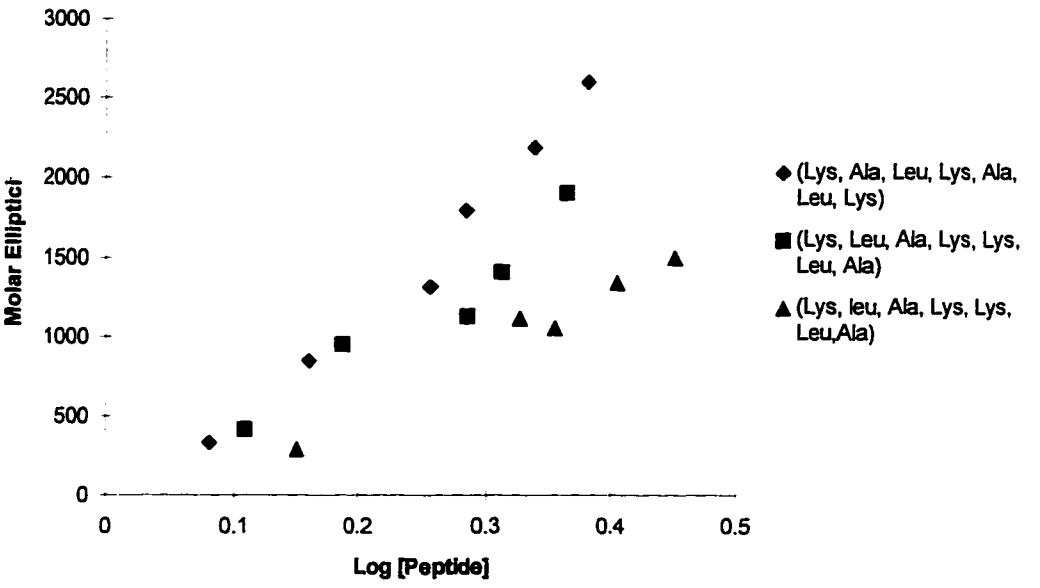

Figure 2.3.4 Log [Peptide] vs. Molar Ellipticity of all the peptides

participate in the aggregation of the peptide. In contrast, the primary leucine zipper for $(Lys,Leu,Ala,Lys,Leu,Ala,Lys)_3$, the leucines for the primary zipper are located on residues 2, 9, 16. The leucine on residue number 2 is not in an α-helix conformation and therefore does not participate in a leucine zipper. The peptide $(Lys,Leu,Ala,Lys,Lys,Leu,Ala)_3$ also has the primary leucine zipper located on the 2, 9 and 16 residue. The greater tenacity of this peptide for aggregation is due to the 160° polar face. Any type of aggregation is helped with nonpolar residues. The greater the face of nonpolar residues, the greater the propensity for nonpolar-nonpolar interactions.

2.3.3 Materials and Methods of Bioassay

All bioassays were done by Martha Juban. Purified peptides were assayed for lytic activity against ATCC strains of Escherichia *coli* 25922, Pseudomonas aeruginosa 27853 and Staphylcoccus aureus 29213. Minimum inhibitory concentrations were determined by the broth microdilution method outlined for aerobic bacteria in NCCLS Document M7-A2, second edition.

Peptide solutions were prepared as a serial 2:1 dilutions from a 512 μg/mL to 2 μg/mL. Bacterial cultures were grown to mid-log phase in nutrient broth and visually standardized to a 0.5 McFarland turbidity tube before dilution. 5×10^4 cells in 50 μL of broth were added to an equal volume of peptide solution in sterile wells, and incubated overnight. The MIC is the lowest concentration of peptide that completely inhibits growth of the organism as detected by the unaided eye.

2.4 Experimental

2.4.1 General Methods

The peptides were synthesized on a Milligen 9050 peptide synthesizer using orthogonally protected amino acids. The α amines were protected using FMOC and the ε–amines on the lysines were protected with t-BOC. The carboxylate ends of the amino acids were activated as an OPfp ester. The resin used was PAL-PEG-PS and all amino acids were weighed to have a 4 fold excess compared to the resin substitution level. HPLC was conducted on a Waters 600E instrument. The analytical and prep methods used a Waters C4 cartridge column while the prep fractions were checked using a Vyadac C-18 column. The mobile phase was a gradient of double distilled water and acetonitrile. CD concentration studies were carried out on a Aviv Model 62DS CD spectrometer. The pathlengths of the cells varied from 0.001 cm at high concentration to 0.01 cm at lower concentrations. All concentration studies were carried out using 2.5mM potassium phosphate buffer pH= 7.45.

2.4.2 Solid Phase Peptide Synthesis

The procedure for the synthesis of a peptide via solid phase peptide synthesizer follows a repetitive scheme. After the PAL-PEG resin is placed in a column, there is an initial washing of the resin using DMF at 5mL/ min which cleans the resin/amino acid. This is followed by a piperidine wash for 10min at 5ml/min. Since piperidine is a base, the purpose of it is to remove the FMOC protecting group of the α-amine on the amino acid anchored on the resin. After this step, the resin/peptide is washed again with DMF for 12 min (at 5mL/min). This needs to be done in order to insure that residual piperidine is removed. While the resin is being washed, the next amino acid is being

dissolved in DMF and 1-hydroxybenzotriazole (HOBT). The HOBT improves coupling yields. The amino acid, after being dissolved in the DMF/HOBT, is delivered to the resin where it is recycled through the resin for 1 hour. This is followed by an 8 minute DMF wash to remove the excess amino acid present in the system. The above is repeated until the peptide has been completed. After the final amino acid is placed on the peptide, there is a 12 minute DMF wash at 5 mL/min and a 15 min DCM wash. At this point the peptide/resin combination is taken off of the synthesizer and is manually washed with MeOH in order to shrink the resin and it is filtered and dried in a high vacuum desicator. After drying the peptide is cleaved using reagent B. Reagent B is made by combining 8.8 mL trifluoroacetic acid, 0.5 mL phenol, 0.5 mL water, 0.2 mL of triisopropylsilane while bubbling Ar through the system. This is added to the peptide/resin and stirred for 4 hours and the mixture was filtered to remove the peptide from the resin. Again two methods were used to purify the peptide. In the first method, the solution containing the peptide was dropped into cold diethyl ether where it precipitated as a white solid. The diethyl ether is then placed into Corex tubes and centrifuged at 7000 rpm for 20 minutes at 20°C in order to concentrate the peptide into a pellet. The diethyl ether is poured off and allowed to evaporate. The crude peptide was then dried overnight in a vacuum desicator. After drying, the peptide was dissolved in 0.1 M acetic acid and ran through a Sephadex G-15 column in 100 mg portions. This removes residual organic molecules as well as small peptides which represent failed sequences. The second method involves dissolving the peptide solution in 20% acetic acid and extraction with diethyl ether. The peptide, in the aqueous solution, is frozen and lyophilized. The crude peptide is then further purified using HPLC.

2.4.3 CD Studies

The CD instrument was purged with liquid nitrogen blow-off for 30 minutes before starting. A series of solutions were made with concentrations varying from 40 mg/mL to 8 mg/mL. All solutions were prepared from a stock solution of ~40 mg/mL (this was subsequently corrected via amino acid analysis) using 2.5 mM sodium phosphate buffer at pH=7.3. The pH of the buffered solution was subsequently checked after the addition of the peptide. A CD spectrum was taken from 225 nm to 190 nm at 1 second per point sampling at every 0.5 nm with a bandwidth of 0.7 nm. Two scans of each solution were taken. The resultant milidegrees at 220 nm were converted to molar ellipticity and graphed as a function of log of concentration of peptide in mM.

2.5 Conclusion:

This work demonstrates not only the importance of leucine zippers in aggregation, but also the importance of the placement of the leucine zippers in the α-helical wheel. If not all three leucines are within the α-helical region of the peptide, they will not be able to complete a proper leucine zipper. The result will be a peptide which will have a decreased molar ellipticity due to a decrease in the stabilizing force of the aggregation state which holds the peptide in an α-helical state.

3.1 Uses of Pyrenylalanine

The excited state of pyrene has the unique property of having a high quantum yield and a long lifetime. It also forms an excimer when two pyrenes are within 3 Å from one another due to the overlapping of the π orbitals. Because of this, it has been used as a fluorescent probe. Since 1983, pyrenylalanine (figure 3.1.1) has been used to probe the formation and behavior of peptides and polymer.

Sisido synthesized block polymers of pyrenylalanine with blocks of benzyl glutamates in order to study the spectroscopic properties of the pyrenylalanines.[29] Poly(γ-benzyl dl-glutamate) solubilized the long pyrenylalanine polymer and was studied using CD and fluorescence spectroscopy. Sisido observed tentative evidence that the pyrenyl portion of the peptides arranged itself in a sandwich-like configuration. Homochiral polymers showed reduced excimer formation while racemic polymer had predominant excimer formation. He concluded that descreet arrangement of the peptides reduced excimer formation. Sisido continued his work by doing a more detailed study of the block copolymer of glutamate and pyrene. [30] Using advanced techniques, he isolated the components of fluorescence to show where the excimer formation arises from the random coil and from more ordered systems.

Pyrenylalanines have probed solvent affects on dipeptides. De Schryver synthesized *n*-acetyl-bis(pyrenylalanine)-methylester (both the erythro and threo compounds) in order to determine how solvent effects the arrangement of random coiled peptides. [31] He concluded that hydrogen donating solvents reduce the partial double bond character of the peptide by hydrogen bridging with the solvent making the dipeptides more structured. Hydrogen accepting solvents shifted the dipeptides to a

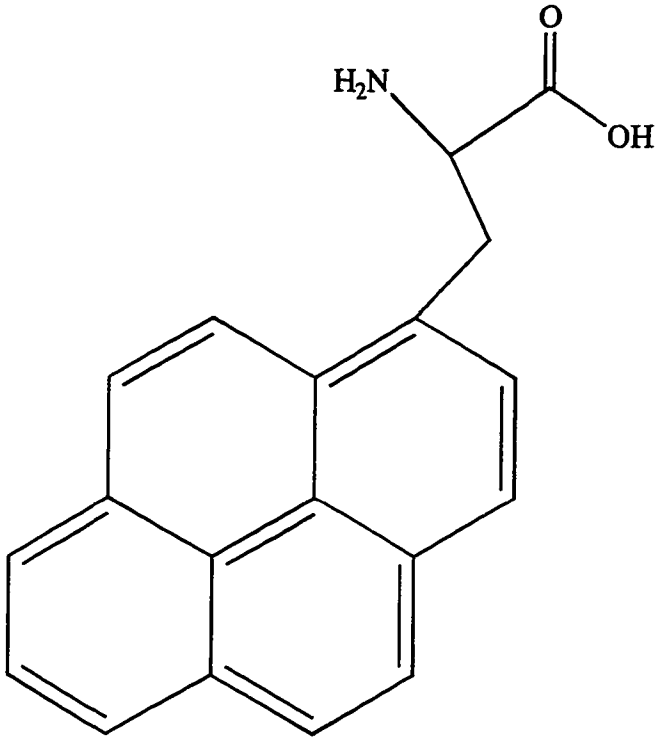

Figure 3.1.1: Pyrenylalanine

more random coil conformation by decreasing intramolecular hydrogen bonding. De Schryver continued his work using both stationary and transient fluorescence techniques to determine how dipeptides behaved in systems. [32] He concluded that the dipeptides are stabilized through intramolecular hydrogen bond formation in the presence of solvents which cannot form hydrogen bonds.

Pyrenylalanine has been used to investigate opiate receptors. In the mid '80s, Costa published a series of papers in which pyrenylalanine was incorporated into the 4 or 5 position in [D-Ala^2, D-Leu^5]enkephalins (heretofore known as DADLE) and its methyl ester. [33] The incorporation of pyrenylalanine made the modified DADLE five times more selective for the δ-receptor. When pyrenylalanine replaced an essential Tyr^1 in an enkephalin, the result showed the pyrenylalanine enkephalin bound to an opiate receptor to a point of inhibiting the Tyr1-containing enkephalin. It is also noted that the methyl ester derivative bound to the μ receptor than to the δ receptor 24 fold more strongly while the C-terminal free analogue of the pyrene enkephalin analogue showed preference for a δ receptor. Incorporation of two pyrenylalanines into an enkephalin analogue in the 1 and 4 or 5 position made the peptide unable to interact with the opiate receptor. [34]

Another aspect of pyrenylalanine investigated involved the idea of photoinduced electron transfer in α-helical backbones.[35] In one paper, p-dimethylanilino acted as an electron donor while pyrenylalanine acted as a photsensitizer with an alanine separating the two groups and coupled to a copolymer of γ-benyl-l-glutamate. The peptide showed electron transfer between the donor and the pyrenylalanine.

Other uses of pyrenylalanine involved the incorporation of it into chiral bilayer membranes that had the property of going from a gel phase to a liquid crystalline phase at 35.2°C. [36] The authors reported that, while in a gel phase the pyrenyl groups arranged in such a way to prevent excimer formation while in the pyrenyl groups randomly ordered in the liquid crystal phase.

Sannamu Lee incorporated pyrenylalanine into an amphipathic/antimicrobial peptide to gain insight into the action of peptides on lipid bilayers. [37] The photophysical results of the peptides interactions on bilayers appeared in a subsequent paper.[38] The amphipathic peptide contained a basic sequence of four amino acids; namely, -L-Leu-L-Ala-L-Arg-L-Leu- in a four quadrad repeat called 4_4. Three different peptides incorporated the pyrenylalanine in the 5th, 7th, and 9th position while one peptide incorporated two pyrenylalanines in the 5th and 9th position. Experiments on these peptides included CD, fluorescent binding studies with DPPC and the authors reported that the labeled peptides existed as a monomer in the liposome layer while as an oligomer in an aqueous layer. The authors also did a quenching study of a tryptophan labeled peptide in a DPPC bilayer and found that iodine did not quench the tryptophan fluorescence. This led the authors to believe that the tryptophan embedded into the nonpolar lipid bilayer while the rest of the peptide lies on the surface of the bilayer. They further concluded that the nonpolar portion of the amphipathic peptide interacted with the lipid bilayer. The authors also observed via CD, that the introduction of the fluorescent side chains in the nonpolar region of the peptide could induce peptide-peptide interactions. This paper clearly demonstrated the use of pyrenylalanine in investigating lipid-peptide and peptide-peptide interaction.

Pyrenylalanine has been used to explore the interaction of two amphipathic α-helical peptides anchored by a bipyridyl group.[39] The peptides incorporated pyrenylalanine in the nonpolar region at the interface between the Leu and Ala. Circular dichroism monitored the interaction of the peptides in both aqueous and MeOH solvents. The authors noted that in an α-helical configuration, the pyrene groups aligned themselves between the two α-helical peptides. MeOH induced a random coil configuration and the pyrenes did not align themselves. A subsequent paper reported further CD and fluorescent data appeared in another paper. [40] Here the authors give evidence of excimer formation under aqueous conditions. The authors also did studies of the denaturation of the covalently attached a-helical bundles using MeOH, heat and guanidine HCl. The covalently bundled peptides exhibited standard denaturation characteristics as evidence through both CD and fluorescent studies. As the peptides became more random coil, an absence of excimer formation occurred.

The use of pyrenylalanine as a fluorescent probe in covalently attached α-helical bundles extended to a 4 covalently attached α-helical bundles. [41] This paper reported both fluorescence and CD spectra. The result showed that the pyrenylalanine, properly placed in the hydrophobic region of the peptide, resulted in excimer formation in aqueous environments. Aqueous environments do promote α-helical structures. Using MeOH as a solvent resulted in little if any excimer formation. The authors stated that the peptide most likely formed a random coil in an MeOH environment and therefore little if any excimer occurred. The authors reported no other evidence that the 4 covalently attached α-helical bundle folded into a bundle structure.

Finally, pyrene explored the nature of leucine zippers in an amphipathic peptide. [42] Garcia-Echeverria used pyrenebutyric acid to label a peptide within its leucine zipper region. CD and fluorescence experiments showed the peptide formed a dimer in aqueous conditions. The fluorescence occurred only if the peptide arranged itself in a parallel dimer formation.

In conclusion the literature clearly shows the usefulness of pyrenylalanine and pyrene products. Through various techniques which depend on the unique fluorescent properties of pyrene, many aspects of the peptides aggregation and structure comes to light.

3.2 Methods for the synthesis of Pyrenylalanine

Various methods have been used to synthesize pyrenylalanine. One of the first involved the formation of an oxalazone with hippuric acid and pyrene carboxaldehyde. This was then hydrogenated and oxidized using phosphorous. [31] This was a racemic mixture though and consequently they were used in this fashion. Figure 3.2.1 illustrates the method for the synthesis of pyrenylalanine.

The most common method for the synthesis of pyrenylalanine is a variation of the above. In this case, the pyrene oxalazone is ring opened using sodium ethoxide and then resolved using (-)-1-phenylethylamine. The result is enantiomercially pure pyrenylalanine. [30] The number of steps in this procedure is six and because the product has to be resolved, the yield on this set of reactions is poor. Figure 3.2.2 illustrates the experimental procedure of this reaction.

Another method that has been used for the synthesis of pyrenylalanine involve creating a template that would only allow the hydrogenation of the precursor

enantionselectively. This molecule first involved the formation of a cyclic dipeptide of glycine and alanine. [34] Chirality of the molecule is introduced with the alanine. The methyl group of the alanine allows for only one face of the pyrene to associate with the palladium. Because of this, only one side of the precursor will be hydrogenated making this enantioselective. Figure 3.2.3 illustrates this reaction set.

Finally, a more interesting method has also been found to produce pyrenylalanine. This involves the use of a acylase. acetyl-DL-Pyrenylalanine was produced using any method of choice. After this Aspergillus acylase was used to deacetylate only the L-pyrenylalanine causing it to precipitate out of solution. This was then collected and used in the experimentation. [40]

3.3 Synthesis of Pyrenylalanine

The synthesis of pyrenylalanine gave us an opportunity to explore the area of glycine templates. Glycine templates are molecules which have a chiral substituent that cause an alkylation to the template to occur enantioselectively. This method offers superior enantioselectively compared to methods which rely on resolution or one in which hydrogenation is directed enantioselectivty. After alkylation, the removal of the enantiomeric directing group is removed and the product is isolated. One such glycine templates is (2R,3S)-(-)-6-oxo-1,4-morphiline-carboxylate or William's template (see figure 3.3.1). The alkylation is directed enantioselectivly by the two chiral phenyl substituents. Once deprotonated, the glycine template will attack an alkyl halide via a backside attack shown in figure 3.3.2.

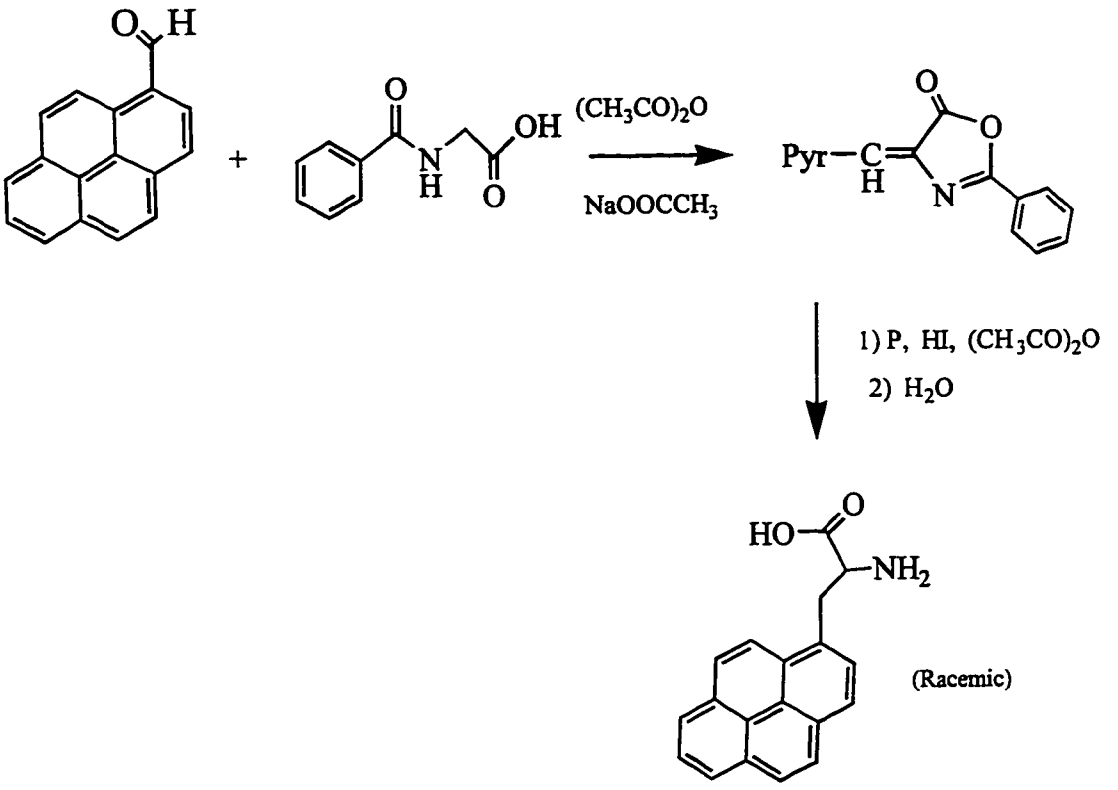

Figure 3.2.1: Synthesis of racemic pyrenylalanine

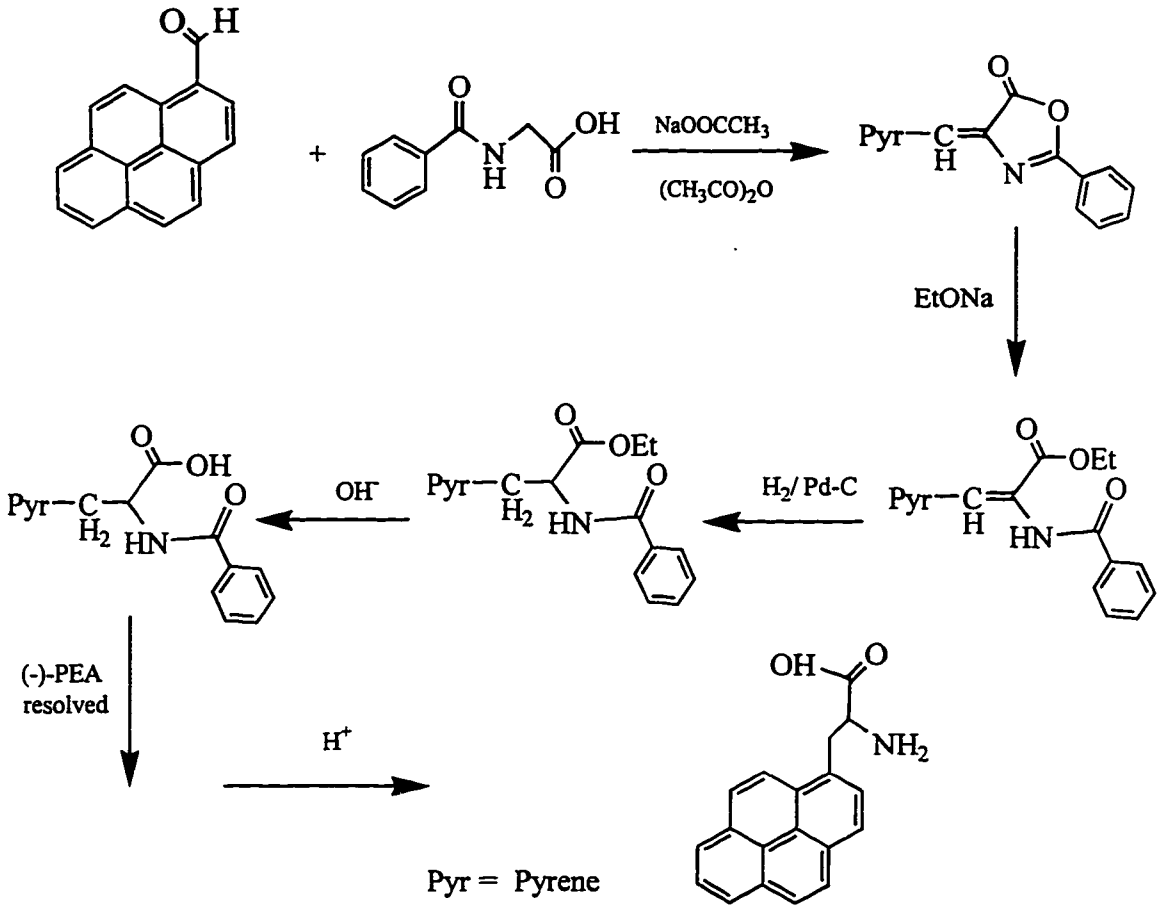

Figure 3.2.2: Synthesis of pyrenylalanine with resolution

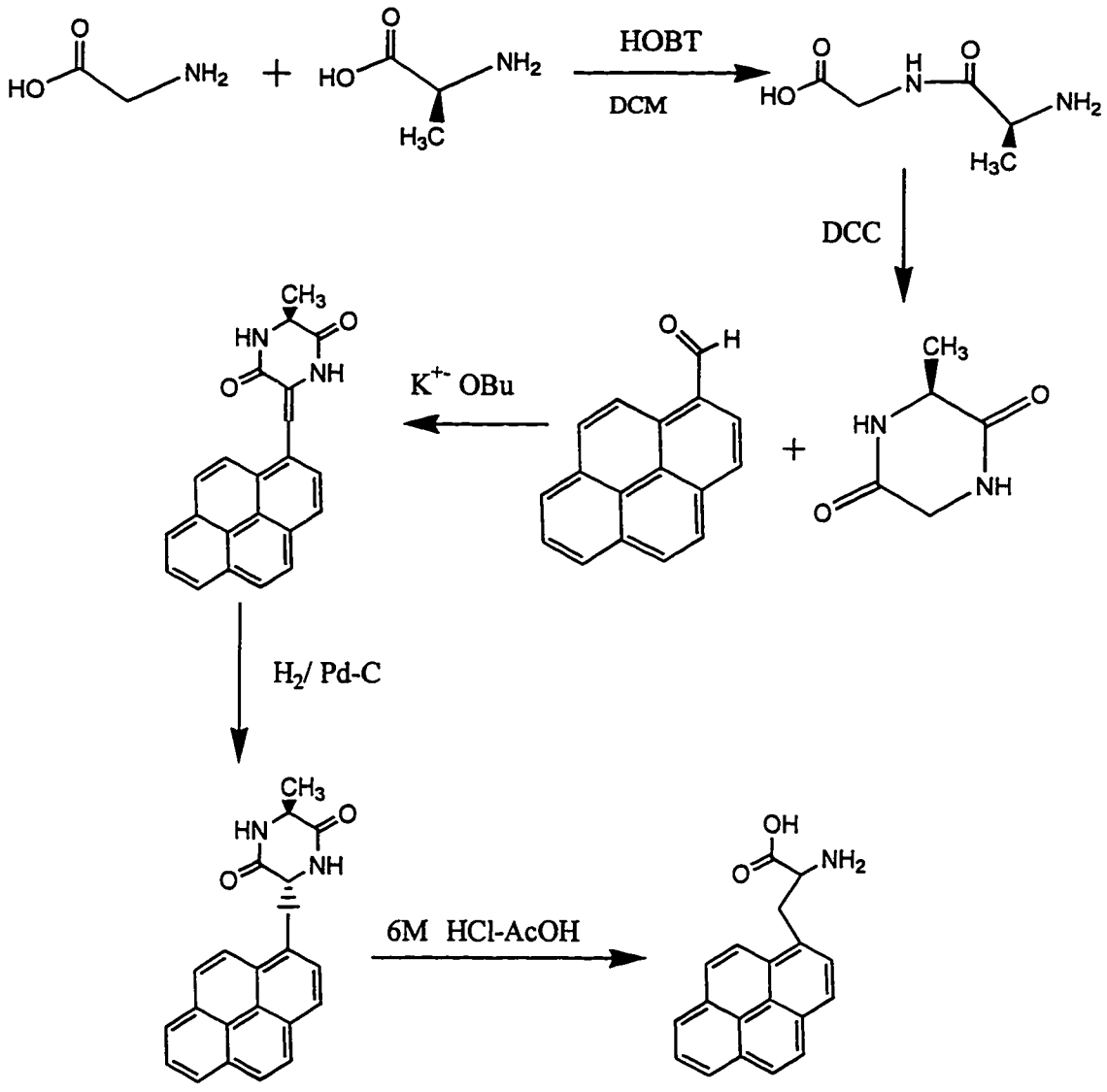

Figure 3.2.3: Synthesis of Pyrenylalanine via enantioselective hydrogenation

Attempted synthesis of pyrenylalanine was a modification of the procedure presented in the literature.[William's, 1990 #93] It involved the following steps. Alkylation of 1-bromomethylpyrene with (2R,3S)-(-)-6-oxo-1,4-morphiline-carboxylate was accomplished by first converting the template to the enolate using Na bistrimethylsylyl amide and then reacting with 1-bromomethylpyrene. The Boc-group was removed with the use of trimethylsilyliodine in an inert atmosphere. The reaction was judged over in about 30minutes via TLC (mobile phase: 50% Hexane, 30% Chloroform 20% Ethyl Acetate). The template was ring opened using 6M HCl. Finally the phenyl rings were to be removed using sodium periodate through oxidation of the phenyl rings to benzaldehyde. Unfortunately, the final step of this reaction did not occur possibility due to the insolubility of the starting material. The solvent conditions for this reaction is THF/H_2O adjusted to a pH of 3. As the reaction continued, the starting material would precipitate. Figure 3.3.3 illustrates the reaction sequence using William's glycine template.

Another template attempted involved a template first synthesized by Seebach. [43] This uses the glycine template1-benzyl-2-*t*-butyl-3-methyl-4-imidazolidinones (see figure 3.3.4). In this case, the enantioselectivity of the molecule is controlled by the chiral *tert*-butyl group. This molecule has the additional advantage of, when the alkylation occurs, the enantioselectivity can be checked by NOESY NMR due to the interaction of the α-proton with the protons on the *tert*-butyl group which is shown in figure 3.3.5. After alkylation, the glycine template was hydrolized to remove the *tert*-butyl group and form the amino acid. Under various conditions attempted, this did not occur. Figure 3.3.6 shows the reaction sequence using Seebach's template.

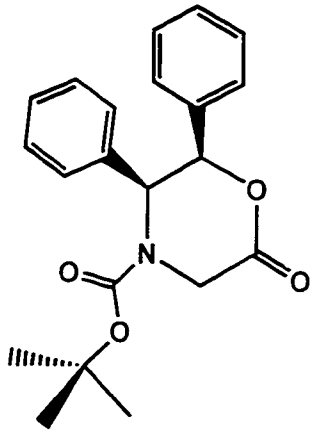

Figure 3.3.1: William's glycine template

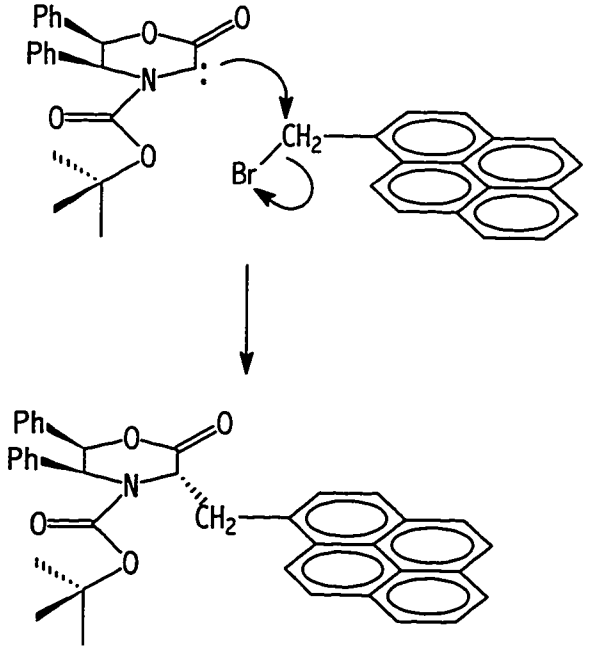

Figure 3.3.2: Alkylation backside attack via glycine template

The failure of all these reactions did not occur in the alkylation, but in the final step of the reaction involving the final formation of the amino acid. It was in the hydrolysis step that failed in these sequences. The reaction sequence that did work used the glycine template invented by O'Donnel. In this template, the hydrolysis step was very facile. Though the reaction does not go enantioselectively, the product was finally synthesized. Figure 3.3.7 illustrates the reaction sequence for the formation of pyrenylalanine.

3.4 Incorporation of Pyrenylalanine into a peptide

The peptide chosen to incorporated the pyrenylalanine was H-(Lys,Leu,Ala, Lys,Lys,Leu,Ala)$_3$-NH_2. The Alanine in the 14th position was replaced with the pyrenylalanine. The synthesis of the peptide containing the pyrenylalanine was accomplished by solid phase peptide synthesis as described in the previous chapter.

Purification of the peptide via HPLC was done under similar conditions as described in the previous chapter. However, since the pyrenylalanine amino acid was racemic, the peptide had to be purified enantiomercially. In order to explain how the peptide was purified enantiomercially, one must understand how a C-4 column works. The nonpolar regions of the peptide bind to the stationary phase of the column upon initial conditions of the mobile phase which is, in this case 90:10 H_20:CH_3CN. As the nonpolar portion of the mobile phase increases, the peptide will then disassociate with the stationary phase allowing it to come out purified. Since different peptides are unique, the percentage of polar/nonpolar mobile phase in which the peptide comes off is also unique. Therefore peptides which contain amino acids that did not couple, and therefore shorter than there parent peptide, will come off at a different time, called the

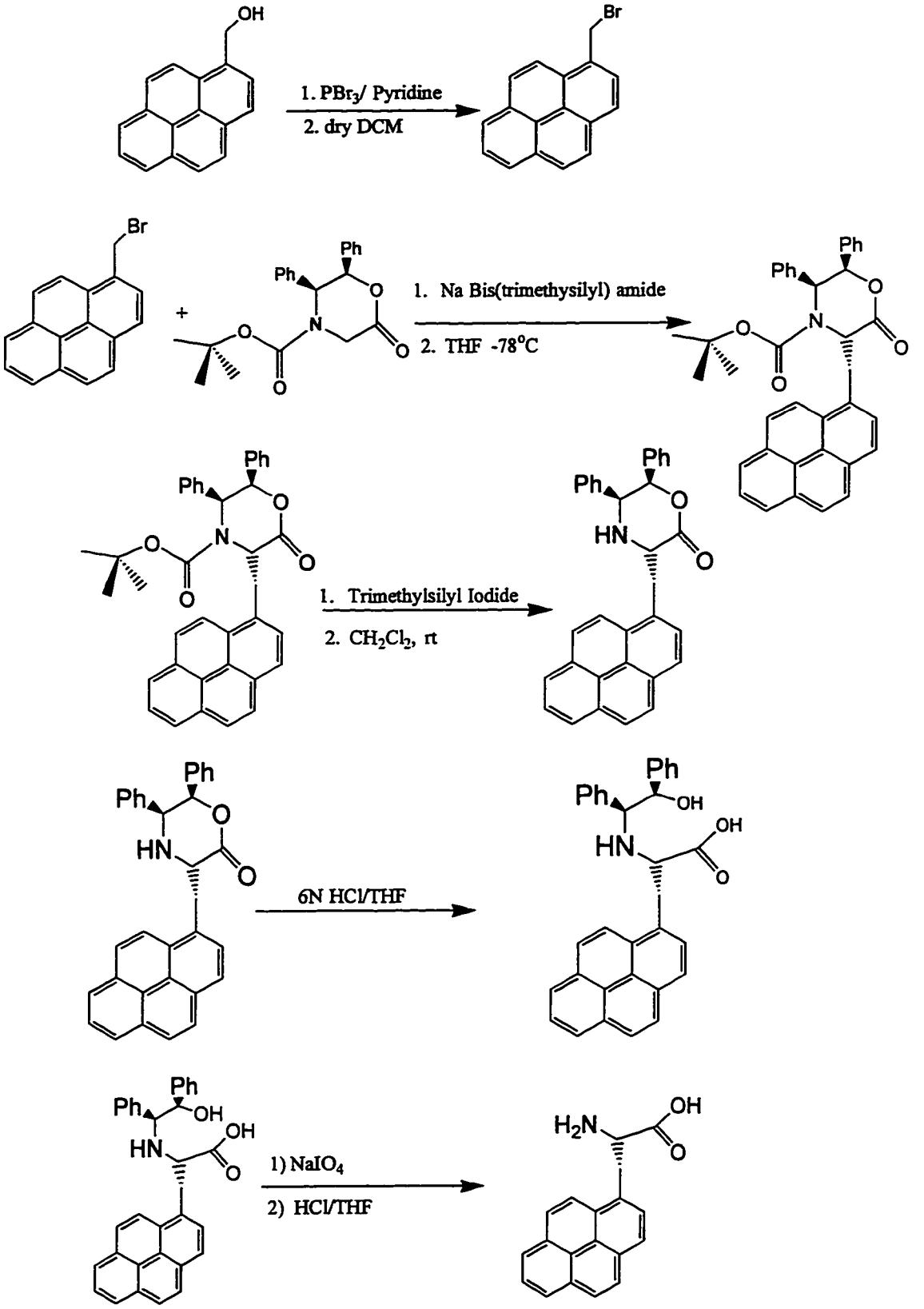

Figure 3.3.3: Attempted Synthesis of Pyrenylalanine using William's glycine template

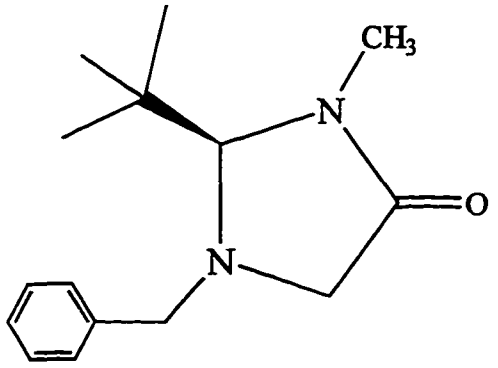

Figure 3.3.4: Seebach's glycine template

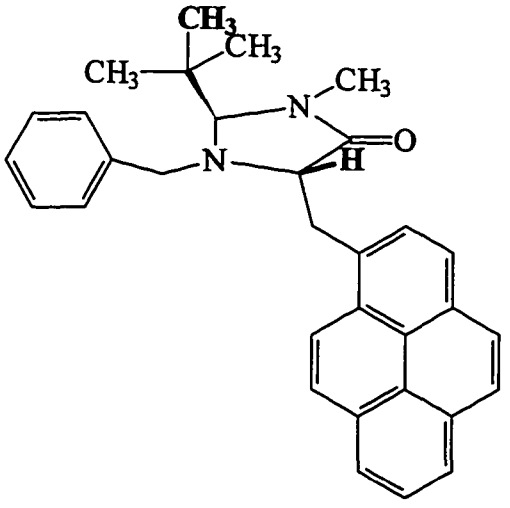

Figure 3.3.5: Alkylated Seebach's glycine template demonstrating how NOESY interactions are used to check the enantioselectivity of the reaction

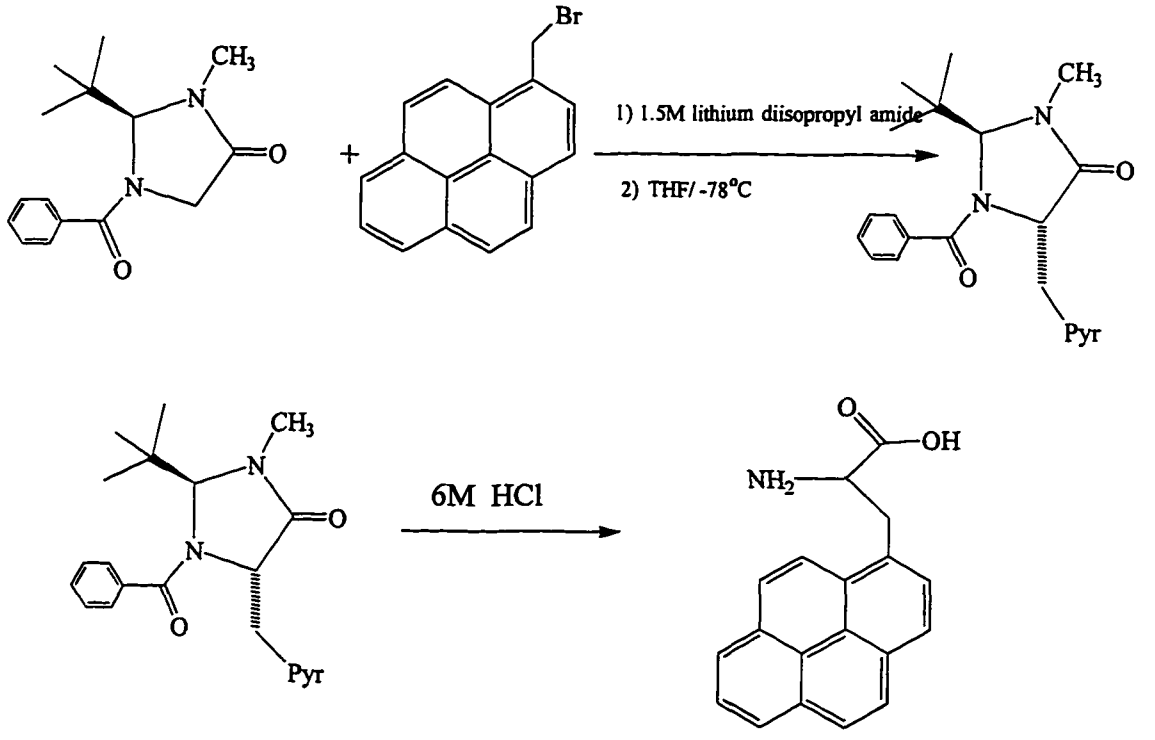

Figure 3.3.6: Attempted synthesis of Pyrenylalanine using Seebach's Glycine template

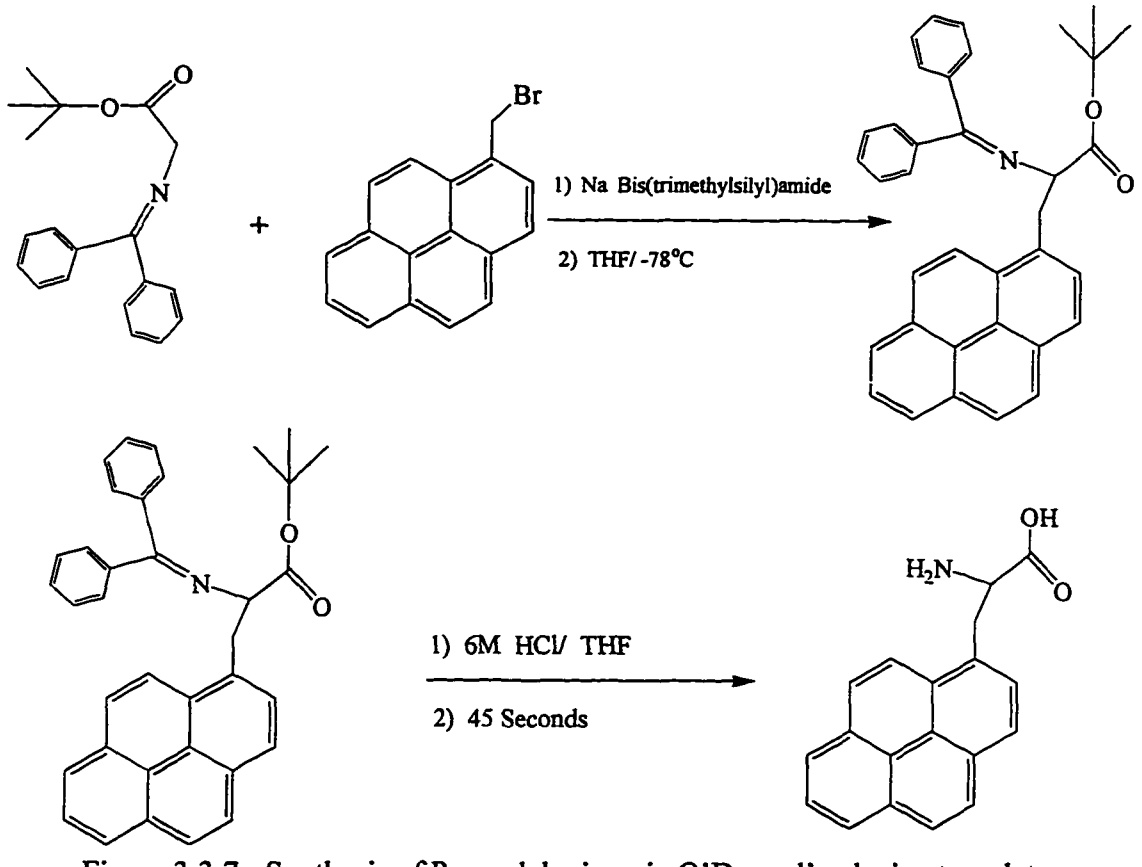

Figure 3.3.7: Synthesis of Pyrenylalanine via O'Donnel's glycine template

retention time, than the completed peptide. What is critical to this system is the actual binding of the peptide to the column stationary phase. The mobile phase 90% H2O/ 10% Acetonitrile causes the peptide to assume an α-helical shape. In this particular case, the peptide synthesized is a mixture containing one with an L-pyrenylalanine and another with a D-pyrenylalanine. When these peptide are α-helical, the one containing the D-pyrenylalanine, is bent as compared to the one containing the L-pyenylalnine. This cause the peptide with the D-pyrenylalanine to have different binding efficiencies than the one with the L-Pyrenylalanine. Therefore the retention time of the D-pyrenylalanine containing peptide will be slightly less than the L-pyrenylalanine containing peptide. This fact was exploited in order to purify the peptides enantiomerically.

3.5 CD and Fluorescence studies of pyrene containing peptide

As the peptides form an α-helical shape, they will tend to aggregate. The question arised as to whether they aggregate parallel or antiparallel to one another. With a pyrenylalanine in the 14th position on the peptide, if the peptides aligned in an antiparallel fashion, then the pyrene may be in close enough proximity to cause the formation of excimer. If the peptides aggregated in an parallel fashion, the pyrenes would not be close enough to form an excimer thus showing no such evidence in the fluorescent studies. The peptide $(Lys,Leu,Ala,Lys,Lys,Leu,Ala)_3$ was used as a model peptide in order to get the solvent conditions appropriate for the peptide containing the fluorescent probe. After incorporation of the fluorescent probe, an absorbance was taken in order to determine if the probe was within the structure and also to determine the concentration of the peptide in various experiments completed (see figure 3.5.1).

The absorbance of the pyrene in the peptide is characteristic of other pyrene containing peptides noted in the literature.

All CD and fluorescent studies were completed in 2.5mM tris buffer. This was done due to a better behavior of peptides in Tris buffer as opposed to phosphate buffer. As stated, the CD's of the peptides were done on with $(Lys,Leu,Ala,Lys,Lys,Leu,Ala)_3$ acting as a model compound. The object of one of the experiments was to find the best solvent conditions for the peptides to exist in an α-helical shape. Figure 3.5.2 shows the CD of the fluorescently labeled peptide in 1M NaCl in tris buffer. The graph is reported in molar ellipticity. Using the formula discussed in the previous chapter, the helicity of the peptide is 81.49%. This affords a good helicity for the peptide to study the possible interactions of the pyrenes in an aggregated state.

Fluorescent study of the peptide was carried out on an SLM model fluorimeter utilizing magic angle. Again this was carried out in 2.5mM tris buffer with 1M NaCl at pH=7.42 using a 35 μL capillary cell. A second study was also carried out in 2.5mM tris buffer without NaCl. Both spectra are shown as figures 3.5.3 and 3.5.4. The peptide is not in an α-helical state without the salt and at these concentrations. Because it is not in an α-helical state, it will not be aggregated in an ordered state. Therefore one can see if there is a difference in the fluorescence between an ordered stated and a nonordered state of peptides.

The fluorescent spectra represented here show the emission spectra when the peptide was excited at different wavelengths. A difference can clearly be seen between both spectra when the peptide was excited at 330 nm. In the system which contained the 1M NaCl, there is a definite tailing in the spectra while the system containing the no

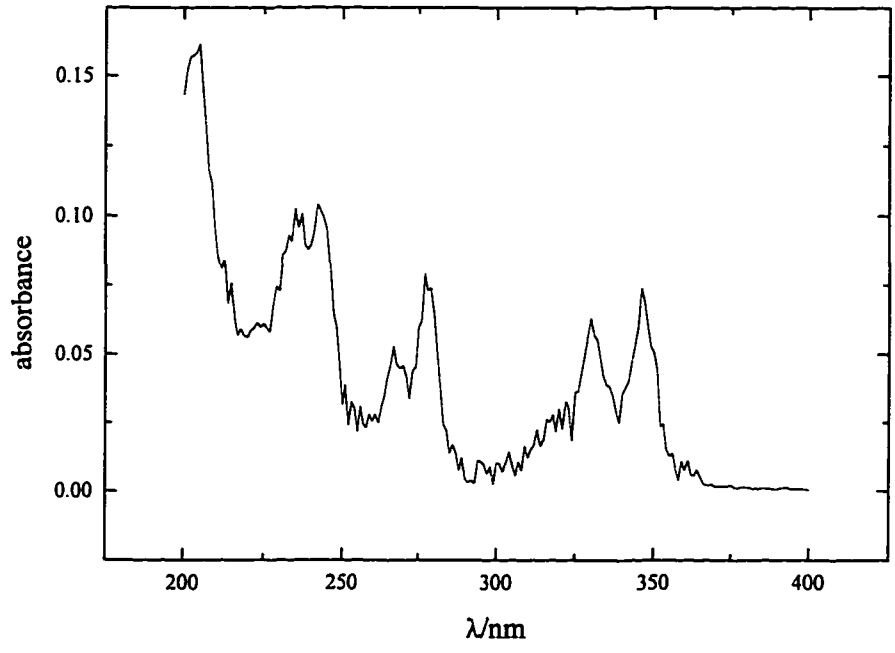

Figure 3.5.1: Absorbance spectra of labeled peptide

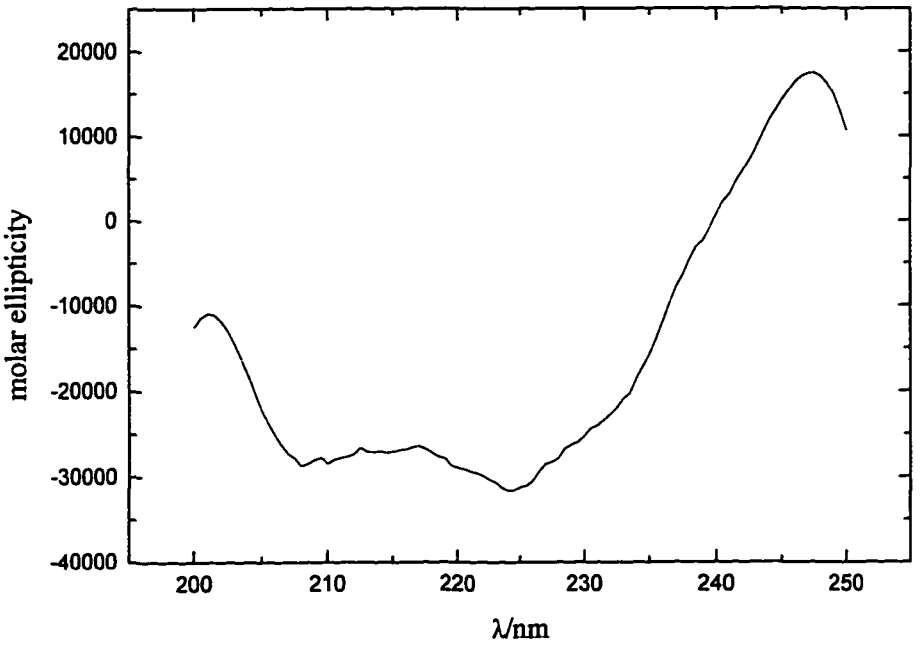

Figure 3.5.2: CD spectra of labeled peptide

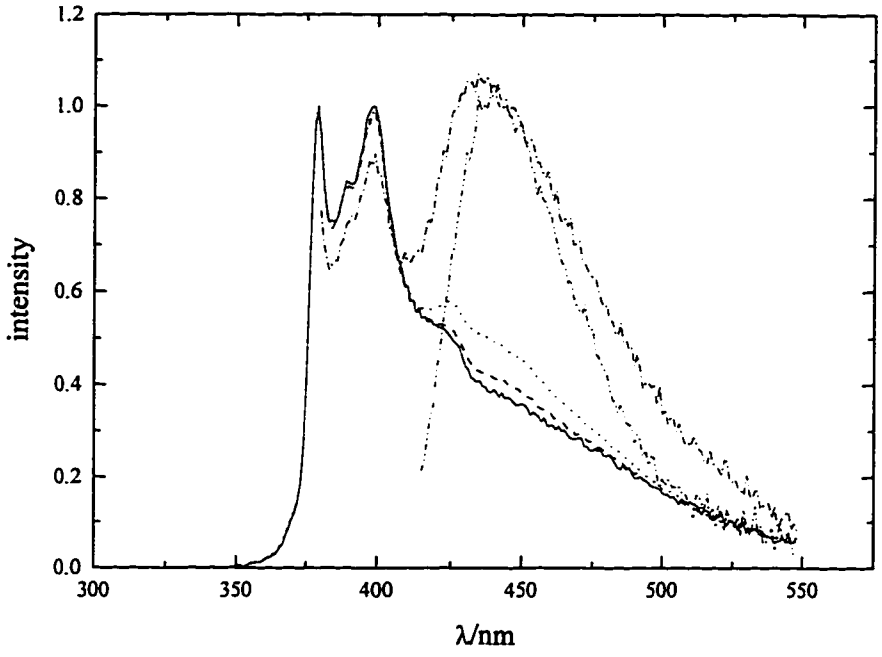

Figure 3.5.3. Emission spectra of labeled peptide 1 M NaCl. ——, 315 nm excitation; -------, 330 nm excitation; ·····, 345 nm excitation; ·-·-·-·, 365 nm excitation; -··-··-, 400 nm excitation.

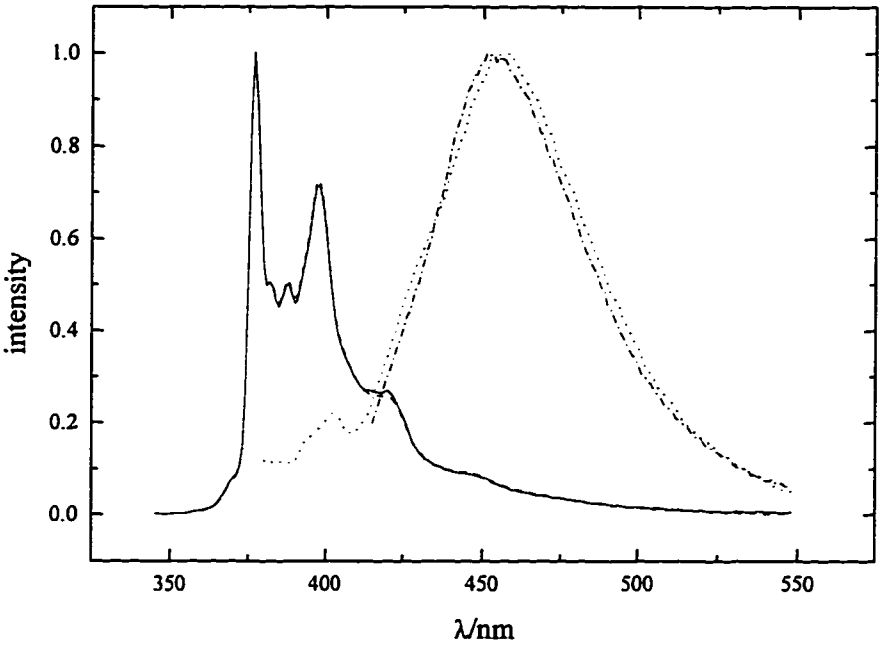

Figure 3.5.4: Emission spectra of labeled peptide 0 M NaCl. ——, 330 nm excitation; ------, 345 nm excitation; ·····, 365 nm excitation; ·-·-·-·, 400 nm excitation.

NaCl there is no such tailing. Because it is being excited at 330 nm, which is considered a low wavelength with pyrene, this is indicative of a ground state emission. Usually in pyrene, a molecule is first excited and then an emission is observed. This excitation is seen when the molecule is excited at wavelengths higher than 365 nm.

3.6: Experimental

3.6.1: Synthesis of 1-bromomethylpyrene

The synthesis of 1-bromomethylpyrene followed a procedure found in a paper by Akiyama with a slight modification.[44] 5.0 g (0.02 mol) of pyrenemethanol was dissolved in 100ml of dry dichloromethane, under Argon, and cooled to 0°C. To this solution was added 0.0908 mL (0.0112 mol) of pyridine. 1.76 mL (0.0187 mol) of PBr_3 was dissolve in dry dichloromethane and added to the pyrenemethanol over a period of 20 minutes. The reaction was then allowed to go overnight. The reaction was then placed in a separatory funnel and cooled double distilled water was added. The organic layer was subsequently washed with water, aqueous sodium bicarbonate and water. The organic layer was then dried with sodium sulfate, filtered and rotovapped. The solid 1-bromomethylpyrene was collected as a yellow powder in an 85% yield; m.p. 141°C; lit m.p. 131-133°C; ^{1}H NMR (200Mhz, $CDCl_3$) 5.25(s,2H) 8.00-8.57(m,9H).

3.6.2: Synthesis of (3R,5R,6S)-4-(*tert*-Butoxycarbonyl)-2,3,5,6-tetrahydro-3-pyrenyl-5,6-diphenyl-1,4-oxazin-2-one.

1.36 g (0.0075 mol) of sodium bis(trimethylsilyl)amide was dissolved in dry THF under Argon and cooled to -78°C using a dry ice/acetone. To this was added slowly in a dropwise fashion, 2.39 g (0.0068 mol) of (3R,5R,6S)-4-(*tert*-

Butoxycarbonyl)-2,3,5,6-tetrahydro-5,6-diphenyl-1,4-oxazin-2-one dissolved in dry THF. After 20 minutes of stirring, 2.0 g (0.0068 mol) of bromomethylpyrene dissolved in dry THF was added dropwise to the above solution and was allowed to stir overnight. Double distilled water was added to the system in order to destroy excess base still present in the system. The product was extracted with diethyl ether and dried over anhydrous sodium sulfate. TLC (mobile phase: 50:30:20 Hexane/Chloroform/Ethyl Acetate) revealed two spots at R_f 0.7 and 0.85. The solvent was removed and the product was recrystallized in refluxing acetonitrile. yield 90%; ^{1}H NMR (200MHz, $CDCl_3$) 1.04(s,9H) 3.54(d,1H) 3.92(d, 1H) 4.08(d, 1H) 4.41(d, 1H) 5.49(d, 1H) 5.87(d,1H) 6.25(d 1H) 6.8-6.94 (m, 10H) 7.7-8.3(m, 9H)

3.6.3: Synthesis of (3R,5R,6S)-2,3,5,6-tetrahydro-3-pyrenyl-5,6-diphenyl-1,4-oxazin-2-one

This reaction follows closely the procedure published by Williams[45] without modifications. 2.0 g (0.0035 mol) of (3R,5R,6S)-4-(*tert*-Butoxycarbonyl)-2,3,5,6-tetrahydro-3-pyrenyl-5,6-diphenyl-1,4-oxazin-2-one was dissolved in dry dichloromethane and stirred under argon. To this was added 1.72 g (0.0085 mol) of trimethylsilyl iodide and stirred for 30 minutes. The reaction was then quenched with 15 mL of water and extracted with dichloromethane. The combined organic layers were washed with 1M sodium thiosulfate. The organic layers were then dried with anhydrous sodium sulfate and rotovapped. Yield 92%; ^{1}H NMR (200MHz, $CDCl_3$) 3.77-3.87 (dd, 1H) 4.27-4.33(dd, 1H) 4.50-4.56(dd, 1H) 4.90(d, 1H) 5.29(dd, 1H) 6.8-7.25(m, 10H) 7.78-8.47 (m, 10H)

3.6.4: Synthesis of N-(1,2-dibenzyl-ethan-2-ol)-pyrenylalanine

This followed closely the procedure of Williams.[45] 1.5 g (0.0030 mol) of (3R,5R,6S)-2,3,5,6-tetrahydro-3-pyrenyl-5,6-diphenyl-1,4-oxazin-2-one was dissolved in a mixture of 25 mL of THF and 50 of 10% HCl and allowed to stir overnight. This was then rotovapped under high vacuum. Yield 95%; ^{1}H NMR (200 MHz, DMF-d_6) 2.78-2.95 (dd, 1H) 3.7-3.5 (dd, 1H) 4.8(d, 1H) 6.86-7.18(m, 10H) 7.99-8.37 (m, 10H)

3.6.5: Attempted synthesis of Pyrenylalanine

1.45 g (0.0028 mol) of N-(1,2-dibenzyl-ethan-2-ol)-pyrenylalanine was dissolved in 25mL of THF. 1.33 g (0.0062 mol) of sodium periodate was dissolved in 45 mL double distilled water adjusted to pH=3 and added to the N-(1,2dibenzyl-ethan-2-ol)-pyrenylalanine solution. This was allowed to stir for three days. After this the flask had a white precipitate which NMR revealed to be starting material.

3.6.6: Synthesis of (2S,5R)-1-benzoyl-2-*tert*-butyl-5-pyenyl-3-methyl-4-imidazolidinone

1.3 mL of 1.5 M LDA was dissolved in THF and placed in a flask under argon and cooled to -78°C using an acetone/dry ice bath. 0.34 g (0.0013 mol) of (2S)-1-benzoyl-2-*tert*-butyl-3-methyl-4-imidazolidinone was dissolved in dry THF and slowly injected into the flask and allowed to stir for 20 minutes. 0.35 g (0.0012 mol) of bromomethylpyrene was dissolved in dry THF and slowly injected into the mixture. After 10 minutes the, the dry ice bath was taken away and the system was allowed to stir

for 2 hours. The reaction was then quenched with double distilled H_2O. The reaction system was then extracted with diethyl ether, dried over anhydrous sodium sulfate and the solvent was removed. Recrystallization was accomplished in ethyl acetate to give a white solid in a 67% yield; m.p. 87°C; ^{1}H NMR (200MHz, $CDCl_3$) 1.01(s, 9H) 2.98(s, 3H) 3.47(s, 1H) 3.85(s, 1H) 4.91-4.93(d, 1H) 5.61(s, 1H) 7.25-7.38(m, 5H) 7.88-8.15(m, 9H)

3.6.7: Attempted synthesis of Pyrenylalanine

0.075 g (0.0002 mol) of (2S,5R)-1-benzoyl-2-*tert*-butyl-5-pyenyl-3-methyl-4-imidazolidinone was dissolved in 6M HCl:glacial acetic acid. This was refluxed at 110°C for 20 hours. NMR revealed starting material.

3.6.8: Synthesis of Schiffbase-*tert*-butoxypyrenylalanine

0.27 g (0.0015 mol) of sodium bis(trimethylsilyl)amide was dissolved in dry THF under argon and cooled to -78°C with an acetone/dry ice bath. 0.44 g (0.0015 mol) of *tert*-Butylglycinate Schiff base was dissolved in dry THF and slowly injected into the solution. This was allowed to stir for 20 minutes. 0.4 g (0.0014 mol) of bromomethylpyrene was dissolved in THF and then slowly injected into the system. This was allowed to stir overnight. The reaction was then quenched with double distilled H_2O, extracted with diethyl ether, dried over anhydrous sodium sulfate and the solvent was removed. Yield 72%; ^{1}H NMR (200 MHz, $CDCl_3$) 1.48 (s, 9H) 3.75-3.84 (dd, 1H) 4.01-4.07 (dd, 1H) 4.44-4.49 (dd, 1H) 6.07 (d, 1H) 6.66-7.50 (m, 10H) 7.8-8.17 (m, 9H)

3.6.9: Synthesis of Pyrenylalanine

1.1 g (0.0022 mol) of Schiffbase-*tert*-butoxypyrenylalanine was dissolved in THF. To this was added a catalytic amount of triisopropylsilane to act as a carbocation scavenger. 6 N HCl was added and an immediate color change was noted. TLC noted one spot R_f =0.0 with a positive ninhydrin test. 1:1 glacial acetic acid:con HCl was added and the mixture was extracted with diethyl ether. The aqueous layer was evaporated overnight to reveal a white crystalline product. This was dissolved in 95%EtOH and, upon neutralization with propylene oxide, a white precipitate formed. 65% yield; ^{1}H NMR (200MHz, DMSO-d_6) 3.33-3.55 (m, 2H) 4.07-4.12 (d, 1H) 7.98-8.47 (m, 9H)

3.6.10: Synthesis of Fmoc-Pyrenylalanine

0.15 g (0.0005 mol) of pyrenylalanine was dissolved in 1:2 solution of 10%Na_2CO_3: Dioxane. 0.192 g (0.0006 mol) of fluorenylmethylcarbonyl sucinimide was directly added to the solution while stirring. The pH of the solution was adjusted to 8 with the slow addition of triethyl amine and the solution was allowed to stir for 30 minutes. The solution was then filtered and then acidified using 1 mol HCl causing a white precipitate to fall out of solution. This precipitate was filtered and dried in a vacuum descicator overnight. TLC (9:1 $CHCl_3$:MeOH) has one spot at R_f= 0.2.Yield 82%; ^{1}H NMR (200MHz, DMSO-d_6) 3.5-3.62(t, 1H) 3.93-4.15(m, 2H) 4.43(t, 1H) 7.11-7.85 (m, 8H), 8.02-8.47 (m, 9H)

3.7: Conclusion

The fluorescently labeled peptide was modeled on Sybyl on an Silicon Graphics Onyx workstation in order to determine how the pyrenes would align when the peptides aggregate in either parallel or antiparallel. If the peptides are aligned in a parallel fashion, the pyrenes would not be in proximity to one another to form an excimer in either a ground or excited state. When the peptides aggregate in an antiparallel fashion, then the pyrenes will align to be able to form an excimer in a ground or an excited state. In fact, the distance between the two pyrenes in an antiparallel aggregation state is between two and six angstoms. However, in the computation study, the peptides were placed in an aggregated state and not aggregated computationally and the aggregated peptides were not minimized.

In conclusion, the placement of one fluorescent probe in a peptide has given a wealth of information. The absorbance spectra showed that the probe was actually placed in the peptide and was used to give an accurate measurement of the concentration of the peptide via Beer's law. The CD spectra of the labeled peptide is the similar to those without a fluorescent label. This is due to the presence of the pyrenylalanine. It also shows that the pyrenylalanine is within the α-helical portion of the peptide. Through solving of the equation mentioned in chapter 2, we found that the peptide is 81% α-helical. Finally by looking at the fluorescence spectra. There shows ground state excimer formation which can only occur when the peptides are aggregated in an antiparallel fashion.

Bibliography

1) Dempsey, C. E. *Biochimica et Biophysica Acta* **1990**, *1031*, 143-161.

2) Houghten, R. A.; Blondelle, S. E. *Biochemistry* **1991**, *30*, 4671-4678.

3) Goto, Y.; Aimoto, S.; Kataoka, M.; Hagihara, Y. *Biochemistry* **1992**, *31*, 11908-11914.

4) Schwarz, G.; Beschiaschvili, G. *Biochemistry* **1988**, *27*, 7826-7831.

5) Goto, Y.; Hagihara, Y. *Biochemistry* **1992**, *31*, 732-738.

6) Ramalingam, K.; Aimoto, S.; Bello, J. *Biopolymers* **1992**, *32*, 981-992.

7) Schwarz, G.; Stankowski, S. *Biochimica et Biophysica Acta* **1990**, *1025*, 164-172.

8) Wasylewski, z.; Kaszycki, P. *Biochimica et Biophysica Acta* **1990**, *1040*, 337-345.

9) Seelig, J.; Beschiaschvili, G. *Biochemistry* **1990**, *29*, 52-58.

10) Subbarao, N. K.; MacDonald, R. C. *Biochimica et Biophysica Acta* **1994**, *1189*, 101-107.

11) Irace, G.; Bismuto, E.; Sirangelo, I. *Biochimica et Biophysica Acta* **1993**, *1146*, 213-218.

12) Andreu, D.; Merrifield, R. B.; Steiner, H.; Boman, H. G. *Proceedings of the National Academy of Science,* USA, **1983**, *80*, 6475-6479.

13) Merrifield, R. B.; Li, Z.-q.; Andreu, D.; Boman, I. A.; Boman, H. G. *The Journal of Biological Chemistry* **1989**, *264*, 5852-5860.

14) Merrifield, R. B.; Fink, J.; Boman, A.; Boman, H. G. *The Journal of Biological Chemistry* **1989**, *264*, 6260-6267.

15) Merrifield, R. B.; Vizioli, L. D.; Boman, H. G. *Journal of the American Chemical Society* **1982**, *21*, 5020-5031.

16) Holak, T. A.; Engstrom, A.; Kraulis, P. J.; Lindeberg, G.; Bennich, H.; Jones, T. A.; Gronenborn, A. M.; Marius, C. G. *Biochemistry* **1988**, *27*, 7620-7629.

17) Boman, H. G.; Mutt, V.; Jornvall, H.; Andersson, M.; Chuanxin, S.; Boman, A.; Lee, J.-Y. *Proceedings of the National Academy of Science,*USA,**1989**, *86*, 9159- 9163.

18) Sipos, D.; Andersson, M.; Ehrenberg, A. *European Journal of Biochemistry* **1992**, *209*, 163-169.

19) Hyde, J. S.; Feix, J. B.; Mchaourab, H. S. *Biochemistry* **1993**, *32*, 11895-11902.

20) Merrifield, R. B.; Fink, J.; Mauzerall, D.; Christensen, B. *Proceedings of the National Academy of Science,* USA, **1988**, *85*, 5072-5076.

21) Guy, H. R.; Raghunathan, G.; Durell, S. R. *Biophysical Journal* **1992**, *63*, 1623-1631.

22) Shai, Y.; Brey, P. T.; Lee, W.-J.; Gazit, E. *Biochemistry* **1994**, *33*, 10681-10692.

23) Fink, J.; Merrifield, R. B.; Boman, A.; Boman, H. G. *The Journal of Biological Chemistry* **1989**, *264*, 6260-6267.

24) Merrifield, R. B.; Wahlin, B.; Boman, I. A.; Wade, D.; Boman, H. G. *FEBS Letters,* **1989**, *259*, 103-106.

25) Sipos, D.; Chandrasekhar, K.; Arvidsson, K.; Engstrom, A.; Ehrenberg, A. *European Journal of Biochemistry* **1991**, *199*, 285-291.

26) Merrifield, R. B.; Wade, D.; Wahlin, B.; Boman, A.; Ubach, J.; Andreu, D.; Boman, H. G. *FEBS Letters* **1992**, *296*, 190-194.

27) Fridkin, M.; Desiderio, D. M.; Dass, C.; Metzger, J. W.; Shalit, I.; Gorea, A.; Bessalle, R. *Journal of Medicinal Chemistry* **1993**, *36*, 1203-1209.

28) Houghten, R. A.; E., B. S. *Biochemistry* **1992**, *31*, 12688-12694.

29) Sisido, M.; Imanishi, Y.; Egusa, S. *Chemistry Letters* **1983**, 1307-1310.

30) Sisido, M.; Imanishi, Y.; Egusa, S. *Macromolecules* **1985**, *18*, 882-889.

31) De Schryver, F. C.; Goedeweeck, R. *Photochemistry and Photobiology* **1984**, *39*, 515-520.

32) De Schryver, F. C.; Van der Auweraer, M.; Goedeweeck, R. *Journal of the American Chemical Society* **1985**, *107*, 2334-2341.

33) Costa, T.; Izumiya, N.; Kato, T.; Aoyagi, H.; Shimohigashi, Y.; Lee, S.; Mihara, H. *FEBS* **1985**, *193*, 35-38.

34) Costa, T.; Izumiya, N.; Kato, T.; Oyagi, H.; Shimohigashi, Y.; Lee, S.; Mihara, H. *International Journal of Protein and Peptide Research* **1987**, *30*, 605-612.

35) Sisido, M.; Tanaka, R.; Inai, Y.; Imanishi, Y. *Journal of the American Chemical Society* **1989**, *111*, 6790-6796.

36) Imanishi, Y.; Sisido, M.; Sasaki, H. *Langmuir* **1990**, *6*, 1008-101?

37) Yoshida, M.; Lee, S.; Mihara, H.; Aoyagi, H.; Kato, T. *Memoirs of the Faculty of Science, Kyushu University* **1988**, *16*, 161-166.

38) Lee, S.; Yoshida, M.; Mihara, H.; Aoyagi, H.; Kato, T.; Yamasaki, N. *Biochimica et Biophysica Acta* **1989**, *984*, 174-182.

39) Fujimoto, T.; Nishino, N.; Mihara, H. *Chemistry Letters* **1992**, 1809- 1812.

40) Mihara, H.; Tanaka, Y.; Fujimoto, T.; Nishino, N. *Journal of the Chemical Society: Perkins Transactions 2* **1995**, 1133-1139.

41) Fujimoto, T.; Tanaka, Y.; Mihara, H.; Nishino, N. *Tetrahedron Letters* **1992**, *33*, 5767-5770.

42) Garcia-Echeverria, C. *Journal of the American Chemical Society* **1994**, *116*, 6031-6032.

43) Seebach, D.; Fitzi, R. *Tetrahedron* **1988**, *44*, 5277-5292.

44) Akiyam, S.; Nakusuji, K.; Nakagawa, M. *Bulletin of the Chemical Society of Japan* **1971**, *44*, 2231-2236.

45) Williams, R. M.; Hendrix, J. A. *Journal of Organic Chemistry* **1990**, *55*, 3723-728.

Vita

Scott Michael Cowell was born on December 16, 1964 in Huntsville, Alabama. He graduated from Grissom High School in Huntsville in May 1983. He received a BA in Chemistry from the University of Alabama in Huntsville in May 1990 and began pursuing his doctorate degree in organic chemistry in the fall of 1990 at Louisiana State University. Currently, he is a candidate for the degree of Doctor of Philosophy in the Department of Chemistry.

DOCTORAL EXAMINATION AND DISSERTATION REPORT

Candidate: Scott M. Cowell

Major Field: Chemistry

Title of Dissertation: Synthesis of Novel Amino Acids with Incorporation into Peptides and Synthesis of Peptides with Novel Aggregation States

Approved:

Mark L. McLaughlin
Major Professor and Chairman

Dean of the Graduate School

EXAMINING COMMITTEE:

John B Hopkins

Robin D. McCarley

Scott L

Andrew W. Ewanick

Date of Examination:

7 November 1996